ACS Sustainable Chemistry & Engineering

pubs.acs.org/journal/ascecg

Research Article

Direct Carboxylation Reactions of Lignin-Derived Biobased Aromatics or Lignin with Carbon Dioxide (CO_2)

Aleksa Kojčinović, Marko Gabrovšek, Edita Jasiukaitytė-Grojzdek, Blaž Likozar,* and Miha Grilc*

Cite This: *ACS Sustainable Chem. Eng.* 2026, 14, 8685−8700

Read Online

ACCESS | Metrics & More | Article Recommendations | Supporting Information

ABSTRACT: Advancing CO_2 utilization and lignin valorization is essential for developing sustainable routes to aromatic chemicals while reducing the dependence on fossil carbon. This study systematically investigates the carboxylation reactivity of 14 lignin-derived hydroxybenzenes using Kolbe−Schmitt and Marasse methodologies to convert CO_2 into value-added aromatic acids. FTIR evaluation of metal phenoxide formation showed that the Kolbe−Schmitt precursor step is highly substrate-dependent and often ineffective for several methoxy- and alkyl-substituted phenols, whereas the Marasse single-pot method with K_2CO_3 provides a more reliable route for all 14 substrates. Comprehensive screening of phenol, catechol, resorcinol, hydroquinone, *o*-, *m*-, and *p*-cresol, anisole, guaiacol, 4-methoxyphenol, syringol, 4-propylphenol, eugenol, and 2-methoxy-4-propylphenol under 150−200 °C, 30 bar of CO_2, and controlled reaction times (1, 2, and 3 h) revealed the broad applicability of the Marasse method. Numerous monocarboxylated products and several dicarboxylated derivatives were obtained, including the first chemical evidence of double carboxylation for resorcinol and extended reactivity for catechol. Methoxyphenols required elevated temperatures, and anisole remained unreactive, confirming the necessity of a free OH group for electrophilic CO_2 insertion. Direct carboxylation of organosolv lignin was investigated, with ^{31}P NMR, 2D HSQC, and SEC analyses demonstrating initial −COOH incorporation at 150 °C. However, this functionalization was accompanied by β-O-4 cleavage followed by dominant condensation and repolymerization reactions at prolonged times or higher temperatures, limiting the overall effectiveness of direct lignin carboxylation under the investigated conditions. Overall, this work delivers the first unified reactivity map for 14 lignin-derived aromatics across varied temperature and time regimes, establishing a foundation for optimizing selective CO_2-based carboxylation toward industrially relevant aromatic acids.

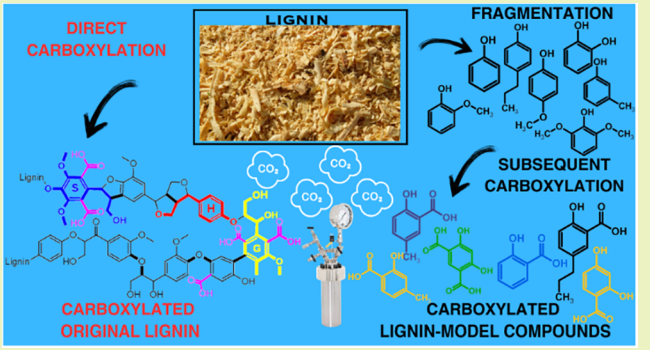

KEYWORDS: *lignin, aromatics, carbon dioxide, carboxylation, carboxylic acids*

1. INTRODUCTION

Over the past few decades, climate change has emerged as a critical issue for the environment, biodiversity, and mankind. Determined to confront this issue, the European Commission has set a goal of reaching net-zero CO_2 emissions by 2050.[1] In attempts to do so, various pathways have been proposed, including energy efficiency, renewable technologies, atmospheric removal of CO_2, long-term storage, etc. Carbon capture and utilization (CCU) techniques have also been identified as key methods, not only for the reduction of CO_2 emissions but also as a means of industrial and lifestyle benefits.

In parallel, biomass valorization has gained recognition as a promising alternative to depleting and environmentally damaging crude oil. Lignocellulosic biomass, particularly lignin, is an abundant yet underutilized source of aromatic hydrocarbons that holds great potential for replacing many oil-derived compounds essential to numerous industries.[2] Besides being essential to all life, carbon fixation reactions are highly advantageous for utilizing CO_2 as, when coupled with biomass, they can form new carbon−carbon bonds and produce compounds with higher energy density.[3] These reaction pathways result in the formation of carboxylic acids, a broad group of compounds with diverse physicochemical properties that are integral to many industries.

Lignocellulosic biomass, consisting of lignin (10−25%), hemicellulose (20−35%), and cellulose (35−50%), is abundantly available in the form of plant and agricultural waste and, as such, serves as an ideal source for industrial applications, as it neither impacts food supplies nor raises ethical concerns.[4] Cellulose and hemicellulose have various technologies that can convert these abundant biopolymers to their sugar monomers,

Received: January 12, 2026
Revised: April 17, 2026
Accepted: April 21, 2026
Published: April 29, 2026

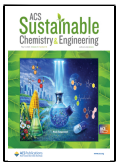

and be used in various industries as biofuels and biochemicals.[5,6] On the other hand, lignin, highly complex in structure and nature, is mainly used in the pulp and paper industry but also inefficiently in power and heat generation. Therefore, this abundant and renewable resource is left poorly valorized and has become of high interest to the research society. In the past decade, various technologies such as pyrolysis, acid/base-catalyzed hydrolysis, hydrotreating, gasification, liquid-phase reforming, etc.[7−11] have been presented as promising routes of depolymerization of lignin to various valuable phenolic compounds. The three precursors or building blocks of lignin (p-coumaryl alcohol, coniferyl alcohol, and sinapyl alcohol) can be easily converted to phenolics such as guaiacol, syringol, catechol, phenol, eugenol, and cresol.[12,13] These aromatic compounds can further undergo a plethora of different upgrading routes to produce a large selection of products. However, carboxylation reactions with these lignin-derived aromatics are rather scarce, as the formation of new C−C bonds is somewhat a challenging task. This highlights both the untapped potential of lignin valorization and the need to further explore carbon fixation strategies to fully exploit its role in the sustainable chemical industry.

The production of alkylphenols has historically relied on petroleum and coal-based routes, though these feedstocks require additional processing due to oxygen deficiency or complex separation steps.[14] On the other hand, lignin from lignocellulosic biomass offers a renewable, oxygen-rich alternative. These lignin-derived aromatics are mostly upgraded via hydrodeoxygenation, demethoxylation, or direct functionalization, while upon preservation of the hydroxyl groups during the conversion, the door to further transformations via CO_2 carboxylation can be opened. Integrating biomass utilization with CO_2 valorization is thus increasingly viewed as a sustainable pathway for producing high-value aromatic chemicals.

The Kolbe−Schmitt carboxylation of phenols and alkylphenols has long served as a cornerstone method for preparing hydroxylated aromatic acids, with salicylic acid being the classic example.[15] Early studies screened diverse substrates, including cresols, catechol, guaiacol, and resorcinol, often under high CO_2 pressures (up to 138 bar), showing that base type, substrate structure, and reaction conditions strongly influence yield and regioselectivity.[16] For instance, p-cresol carboxylation was found to be most efficient with K_2CO_3, giving high yields of corresponding carboxylic acid at 125 °C over long reaction times.[17] Similarly, Mg, Ca, and Ba phenoxides enable near-quantitative conversion to salicylic and dicarboxylic acids at 260 °C and 50 bar CO_2, with the ion size dictating the ortho/para selectivity.[18] Computational studies confirmed that CO_2 preferentially attacks the ortho site via Na−O coordination, explaining experimentally observed ortho dominance.[19] More recent advances include the use of supercritical CO_2, suspension-phase systems in toluene with free phenol recycling, and additives such as carbonates or trisubstituted phenols to shift equilibria toward carboxylated products.[20] Recently, Mohammad et al.[21] demonstrated a suspension-based carboxylation of biomass-derived phenolic sodium salts under moderate CO_2 pressures, achieving high yields of hydroxybenzoic acids and highlighting the influence of precursor additives and mixed phenolic feeds on selectivity. While this approach emphasizes reaction engineering and salt-based activation, systematic structure−reactivity comparisons across a broad substrate range remain limited. Additionally, these refinements demonstrate that while the Kolbe−Schmitt reaction is an old process, its application to alkylphenols remains dynamic, with mechanistic insights and process modifications continuing to expand its efficiency and scope. However, further systematic screening of other lignin-derived alkylphenols, along with process intensification strategies and a deeper understanding of reaction parameters, remains essential to fully exploiting their potential for sustainable chemical production.

While the Kolbe−Schmitt reaction is well established, it typically relies on preformed alkali phenoxides and often requires elevated (supercritical) CO_2 pressures or specific cation effects to achieve high selectivity. In contrast, the Marasse method enables *in situ* generation of reactive phenoxide species using carbonate bases under comparatively milder and more uniform conditions.[15−17,21] This approach minimizes substrate-specific variations arising from isolated salt preparation and allows for a more systematic comparison of structurally diverse lignin-derived aromatics. Therefore, the Marasse methodology was selected to provide a consistent experimental framework for evaluating intrinsic structure−reactivity relationships across all investigated substrates.

The aim of this study was to provide a single, systematic evaluation of carboxylation reactions of 14 different lignin-derived aromatics, focusing on how their structural features influence the activity and selectivity. The Marasse method of carboxylation of hydroxybenzenes was used as a standard methodology for assessing the potential of carboxylation of various lignin-derived aromatics, including hydroxybenzene (phenol), dihydroxybenzenes (catechol, resorcinol, and hydroquinone), methylphenols (*o*-, *m*-, and *p*-cresols), methoxyphenols (anisole, guaiacol, 4-methylphenol, and syringol), and alkylphenols (4-propylphenol, eugenol, and 2-methoxy-4-propylphenol). Primary investigation was focused on the potential preparation of metal phenoxides of corresponding aromatics and assessing the obtained products using the FTIR calibration curve of commercially available PhONa. (monitoring −ONa peak). Direct carboxylation of these aromatics was investigated using only K_2CO_3, as an efficient base for Marasse carboxylation, under 2 different temperatures (150 and 200 °C) and three different reaction times (1, 2, and 3 h). These results provided a large amount of experimental points (84 carboxylation reactions) and the assessment of all potentially obtained mono- and dicarboxylated corresponding aromatics. To complete the study, direct carboxylation of pure lignin was studied, and the obtained products were investigated using size exclusion chromatography (SEC), phosphorus nuclear magnetic resonance (^{31}P NMR), and 2D heteronuclear single quantum coherence NMR (HSQC). This study acts as the first and only research assessing such a large amount of various lignin-derived aromatics for direct carboxylation, using CO_2 as a reactant.

2. EXPERIMENTAL SECTION

2.1. Materials

All the reactants, precursors, and gases have been purchased from commercial suppliers and have been used on an as-is basis, without any further purification. For the preparation of metal phenoxides, along with the lignin-based aromatics, solid sodium hydroxide NaOH was used (≥98%, pellets (anhydrous), Honeywell Fluka, Charlotte, NC, USA), as well as toluene (≥99.9%, Merck Emsure KGaA, Darmstadt, Germany). The assortment of lignin-derived aromatics included phenol PHE, catechol CAT (>99%, Thermo Fisher

https://doi.org/10.1021/acssuschemeng.6c00430
ACS Sustainable Chem. Eng. 2026, 14, 8685−8700

Scientific, Waltham, MA, USA), resorcinol RES (>99.0%, Thermo Fisher Scientific, Waltham, MA, USA), hydroquinone HYD (99%, Thermo Fisher Scientific, Waltham, MA, USA), *o*-cresol *o*-CRE (≥98%, Sigma-Aldrich, St. Louis, MO, USA), *m*-cresol *m*-CRE (99%, Sigma-Aldrich, St. Louis, MO, USA), *p*-cresol *p*-CRE (99%, Sigma-Aldrich, St. Louis, MO, USA), anisole ANI (≥99%, Honeywell Fluka, Charlotte, NC, USA), guaiacol GUA (>98.0%, Carl Roth, Karlsruhe, Germany), 4-methoxyphenol 4MOP (≥98.0%, Thermo Fisher Scientific, Waltham, MA, USA), syringol SYR (99%, Sigma-Aldrich, St. Louis, MO, USA), 4-propylphenol 4PP (≥97%, TCI Tokyo Chemical Industry, Tokyo, Japan), eugenol EUG (99%, Thermo Fisher Scientific, Waltham, MA, USA), and 2-methoxy-4-propylphenol 2MO4PP (≥99%, Sigma-Aldrich, St. Louis, MO, USA). For the preparation of the sample for ^{1}H NMR, deuterated water D_2O was used as a solvent (99.9%, Thermo Fisher Scientific, Waltham, MA, USA) and internal standard sodium formate (99.0%, Carl Roth, Karlsruhe, Germany). Isolation of lignin was catalyzed with sulfuric acid (H_2SO_4, 95−98%, Sigma-Aldrich, St. Louis, MO, USA). Preparation of samples for size exclusion chromatography and phosphorus NMR involved the following chemicals: pyridine (≥99.9%, Sigma-Aldrich, St. Louis, MO, USA), dimethyl sulfoxide DMSO (≥99.7%, Sigma-Aldrich, St. Louis, MO, USA), *N*-hydroxy-5-norbornene-2,3-dicarboxylic acid imide NHND (>99.0%, TCI Tokyo Chemical Industry, Tokyo, Japan), chromium(III) 2,4-pentanedionate (>98.0%, TCI Tokyo Chemical Industry, Tokyo, Japan), and 2-chloro-4,4,5,5-tetramethyl-1,3,2-dioxaphospholane TMDP (95%, Sigma-Aldrich, St. Louis, MO, USA).

2.2. Experimental Reaction Procedures

2.2.1. Extraction of Lignin. Lignin was isolated from beech sawdust (42 g, <24 mesh, oven-dried at 105 °C for 24 h) using 50 vol % ethanol/water at a 1:7 (w/v) ratio. To catalyze the reaction, 1% H_2SO_4 (based on dry weight) was introduced into the mixture. Extractions were performed in a Parr 4575A 500 mL cylindrical stainless steel batch reactor at 160 °C for 1 h and at 200 rpm. Prior to the heating, the vessel was flushed twice and pressurized with nitrogen to 2 bar. The reaction was stopped by immersing the reactor in an ice bath. Solid residues were separated by filtration and rinsed with 257 mL of a 4:1 ethanol/water solution heated to 60 °C to release lignin retained on the wood particle surfaces. The obtained solids were then dried at 105 °C for 48 h. Lignin was recovered by adding 3-fold excess of distilled water, after which the precipitate was collected via centrifugation (10 min, 4500 rpm), repeatedly washed with distilled water, and freeze-dried.

2.2.2. Preparation of Metal Phenoxide and Direct Carboxylation Reactions. The preparation of metal phenoxide was carried out using the reflux method, as described in our previous publication.[22] The procedure involved dissolving lignin-derived aromatics (individually) into 10 mL of toluene, while NaOH was introduced into the round-bottom flask with 30 mL of toluene. Half of the amount of prepared aromatic solution was introduced immediately, and the second half after 1.5 h. The synthesis was carried out for 3 h under reflux at 120 °C, after which it was vacuum-filtered to obtain solid metal phenoxides, which were then dried overnight in vacuum at 40 °C. Successful formation of metal phenoxides was confirmed by FTIR spectroscopy through monitoring of the characteristic −ONa stretching band (~3550 cm^{-1}), using a previously established calibration curve based on Ph:PhONa mixtures.[22] The disappearance of the phenolic −OH band and the appearance of the corresponding −ONa vibration confirmed effective deprotonation. Due to the solid-state nature and hygroscopic behavior of the phenoxides, quantitative chromatographic analysis was not feasible.

Direct carboxylation of lignin-derived aromatics included introducing 0.25 mol of each aromatic compound into the Parr 2500 Multi Reactor System (Parr Instruments Company, Moline, IL, USA), along with K_2CO_3, while keeping the 2:1 ratio of potassium ions to −OH groups. After the contents were introduced into the reactor, the reactor itself was purged three times with 10 bar of CO_2, and then 30 bar of CO_2 was released into the reactor. The 30 bar CO_2 pressure was chosen as a standard procedure, as our previous study[23] has shown a significant negative effect of CO_2 pressure below 20 bar, while the literature-suggested supercritical CO_2 conditions require more complex operational system. The desired temperature (150 or 200 °C) was set with a heat-up rate of 7 °C min^{-1}, and once the temperature was reached, the start of the reaction was noted. After the desired reaction time was reached (1, 2, or 3 h), the reactors were cooled to room temperature, and their contents were dissolved in 5 mL of 5 mM H_2SO_4.

2.3. Analytical Methods

2.3.1. Size Exclusion Chromatography (SEC). The analysis of the lignin carboxylation reaction was done with size exclusion chromatography (SEC). This method allowed for quantification of the average molecular weight distribution (M_w), average number of monomer units (M_n), and dispersity ($Đ$). The samples for SEC were initially dissolved at a concentration of 200 mg in 2 mL pyridine, stirred at 300 min^{-1}, and heated to 40 °C overnight. They were then filtered through a 0.2 μm syringe filter to remove the unreacted and undissolved potassium carbonate. The dissolved lignin was then precipitated in cold distilled water and subsequently centrifuged at 9500 min^{-1} for 10 min. All samples were then washed three times with distilled water to remove pyridine residues. Finally, all samples were freeze-dried and used for analysis.

SEC analysis was performed on a Thermo Fisher Scientific Ultimate 3000 system (Ultimate 3000, Thermo Fisher Scientific, Massachusetts, US) equipped with a refractive index detector (differential refractometer, RI) set to 40 °C with 10 Hz collection rate using a Polargel 8 μm Polargel-M 7.5 mm × 300 mm column with 0.05 M LiBr in DMSO as an eluent at a flow rate of 0.5 cm^3 min^{-1} and column oven temperature of 60 °C. Calibration was made with Pullulan standards (Polymer Standards Service; PSS) with molecular weights in the range from 194 kDa to 342 Da. The chromatographic data were processed with PSS WinGPC Unity software.

2.3.2. ^{31}P Nuclear Magnetic Resonance (^{31}P NMR). Analysis of pure lignin carboxylation reaction products was also done with phosphorus nuclear magnetic resonance (^{31}P NMR). This method allowed for quantification of various −OH groups (aliphatic, syringyl, guaiacyl, and phenolic) as well as carboxylic −COOH groups, present on the lignin structure. After cooling down and opening the reactor, the reaction contents were acidified with 5 mL of 5 mM H_2SO_4 to protonate the −ONa and/or −COONa groups, followed by overnight vacuum drying. Between 300 and 315 mg of dry sample were mixed with 4 mL of pyridine and deuterated chloroform solution (1.6:1) and stirred overnight at 200 rpm. All of the lignin content was successfully dissolved, while the potassium carbonate stayed in solid form on the bottom of the vial. The next step involved withdrawing 400 μL of the lignin solution and adding 100 μL of internal standard (18 mg/mL NHND (*N*-hydroxy-5-norbornene-2,3-dicarboxylic acid imide) and 5 mg/mL chromium(III) 2,4-pentanedionate), also stirred overnight at 200 rpm. The last step involved adding 100 μL of reagent TMDP (2-chloro-4,4,5,5-tetramethyl-1,3,2-dioxaphospholane), stirring for 90 min at 200 rpm, and analyzing the sample immediately on the NMR machine (Bruker 600 MHz ORO600). The obtained spectra were processed using Mnova software: the reference point (always the second peak in the chromatogram), NHND, was set at 151.86 ppm and normalized to 1; baseline was adjusted with manual correction (multipoint baseline correction using Whittaker algorithm), and the peaks of interest were integrated. The peaks of interest for hardwood lignin include: 152.29−151.52 ppm of internal standard (IS), 150.00−145.43 ppm of aliphatic −OH, 143.10−142.35 ppm of syringyl −OH, 140.35−137.32 ppm of guaiacyl −OH, and 135.89−134.14 ppm of −COOH.

2.3.3. 2D Heteronuclear Single Quantum Coherence (HSQC). 2D heteronuclear single quantum coherence (HSQC) NMR spectra were recorded using a Bruker AVANCE NEO 600 MHz NMR spectrometer equipped with BBFO probe following the protocol reported by Tran et al.[24] Approximately 85 mg of lignin sample was dissolved in 0.6 mL of DMSO-d6, which was also used as

https://doi.org/10.1021/acssuschemeng.6c00430
ACS Sustainable Chem. Eng. 2026, 14, 8685−8700

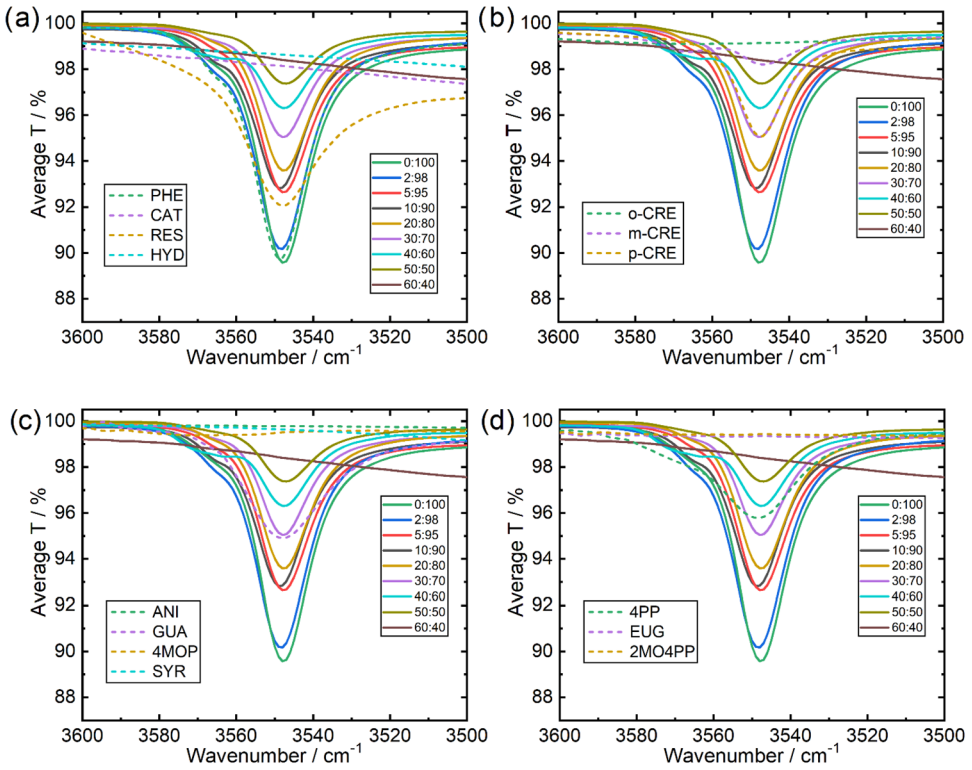

Figure 1. FTIR measurements of prepared sodium-based aromatic salts, including phenol (PHE), catechol (CAT), resorcinol (RES), and hydroquinone (HYD) (a); *o*-cresol (*o*-CRE), *m*-cresol (*m*-CRE), and *p*-cresol (*p*-CRE) (b); anisole (ANI), guaiacol (GUA), 4-methoxyphenol (4MOP), and syringol (SYR) (c); 4-propylphenol (4PP), eugenol (EUG), and 2-methoxy-4-propylphenol (2MO4PP) (d).

an internal chemical shift reference point (δC 39.5;δH 2.50 ppm). HSQC spectra analysis, assignment of the different lignin cross-signals, and calculations were made following the reported procedure.

2.3.4. ^{1}H Nuclear Magnetic Resonance. Quantification of the obtained products from all the carboxylation reactions of lignin-derived aromatics was done with proton nuclear magnetic resonance (^{1}H NMR). After the acidification and dissolving step of the obtained solid products, 2 mL was withdrawn and mixed with 5 mL of deuterated water (D_2O) and 0.01 g of sodium formate, which acted as an internal standard. ^{1}H NMR spectra were measured on a Bruker AVANCE NEO 600 MHz (Bruker, Billerica, Massachusetts, United States of America) spectrometer at 25 °C. A mixture of D_2O, H_2O, and DMSO-d6 was used as a solvent. Chemical shifts were reported on the ppm scale; coupling constants are reported in Hz. Sodium formate was used as an internal standard and reference (8.375 ppm) to give yields of the reactions. Peak multiplicity was reported using the following abbreviations: m, multiplet; d, doublet; t, triplet; and dd, doublet of doublets. The obtained yields were determined from ^{1}H NMR spectra and calculated on a molar yield basis, from the ratio of integrals of the internal standard sodium formate and the characteristic signals corresponding to reactants and products. Structural identification of mono- and dicarboxylated products was performed by analysis of chemical shifts, signal multiplicity, and comparison with literature data. In selected cases, signal patterns corresponding to ortho- or para-substituted aromatic acids were used to confirm regioisomer formation. Representative spectra and detailed peak assignments are provided in the Supporting Information.

3. RESULTS

3.1. Preparation of Sodium-Based Aromatic Salts

For successful carboxylation of aromatics, the first step is necessary: reacting the aromatics with a base (carbonates or hydroxides) and forming metal-oxide aromatic salts.[25] Deprotonation of the phenolic −OH group by a strong base generates a reactive phenoxide species, which subsequently acts as the nucleophile in the carboxylation step. As previous studies and the literature suggested, sodium hydroxide, due to its strong basicity, represents one of the best possible candidates for various aromatics. The first step of Kolbe-Schmitt-type reactions included heating the aromatics with excess NaOH, suspended in toluene, and connected to a reflux. This setup, in contrast to the open-beaker method, avoided evaporation of the solvent and simultaneously compounds of interest, or their potential charring.[22] Figure 1 shows FTIR analyses of obtained products from reacting NaOH with 14 different lignin-derived aromatics, under 120 °C, for 3 h. As previously reported,[22] a calibration curve constructed from defined phenol-to-sodium phenoxide (Ph:PhONa) ratios was used to monitor the characteristic −ONa stretching band at 3550 cm^{-1}. The intensity of this band directly reflects the extent of phenolic deprotonation and thus the degree of metal phenoxide formation. While this FTIR-based approach does not provide the quantitative precision of chromatographic techniques such as HPLC, it represents a suitable method for assessing phenoxide formation in the solid state. Accurate quantification by HPLC is inherently limited because dissolution leads to the reprotonation of the phenoxide species, preventing reliable measurement of the deprotonated form. Moreover, obtaining a fully homogeneous solid sample of metal phenoxides is experimentally challenging, further complicating rigorous quantitative analysis. For these reasons, the calibration curve was employed as a semiquantitative tool to compare relative −ONa formation across substrates rather than to determine exact conversion values, while also providing insightful information for the potential second step of the

https://doi.org/10.1021/acssuschemeng.6c00430
ACS Sustainable Chem. Eng. 2026, 14, 8685−8700

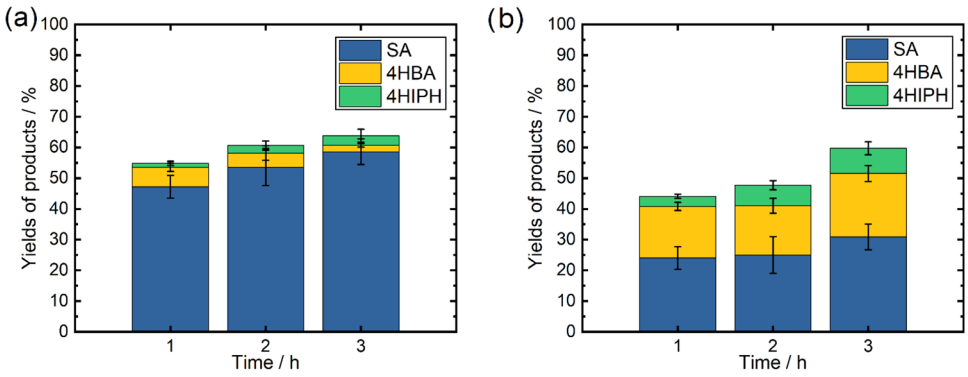

Figure 2. Yields of obtained products salicylic acid (SA), 4-hydroxybenzoic acid (4HBA), and 4-hydroxyisophthalic acid (4HIPH), obtained after 1, 2, and 3 h, under 150 °C (a) and 200 °C (b) (30 bar of CO_2, 2.5 mmol of PHE, 2.5 mmol of K_2CO_3, 600 rpm).

Kolbe−Schmitt reaction, involving the carboxylation of the prepared sodium phenoxide substrate.

Figure 1a shows the −ONa peaks of prepared mono- and dihydroxybenzenes: phenol-, catechol-, resorcinol-, and hydroquinone-sodium salt analogues. It can be seen that phenol (PHE, dashed green line) shows around 100% presence of the −ONa peak, catechol (CAT, dashed purple line) around 42%, resorcinol (RES, dashed brown line) around 96%, and hydroquinone (HYD, dashed blue line) below 40%. Figure 1b shows −ONa peaks obtained from methylphenols: *o*-cresol (*o*-CRE, dashed green line) with amounts below 40%, *m*-cresol (*m*-CRE, dashed purple line) around 42%, and *p*-cresols (*p*-CRE, dashed brown line) with around 70%. Figure 1c shows −ONa peaks obtained from methoxylphenols: anisole (ANI, dashed green line), 4-methoxyphenol (dashed brown line), and syringol (dashed blue line) with amounts significantly below 40% (the lowest concentration used in the calibration curve), and probably close to 0% of the obtained −ONa bond. Lastly, guaiacol (dashed purple line) shows around 71%. Figure 1d shows −ONa peaks obtained from alkylphenols: 4-propylphenol (4PP, dashed green line) with amounts around 65%, while eugenol (EUG, dashed purple line) and 2-methoxy-4-propylphenol (2MO4PP, dashed brown line) show −ONa peaks, significantly below 40%, probably because of the unsuccessful reaction and no metal phenoxide was obtained.

The results reveal a clear dependence of phenoxide formation on the substitution pattern and electronic effects. Among the hydroxybenzenes, phenol and resorcinol exhibit nearly complete conversion to their sodium salts, whereas catechol and hydroquinone show substantially lower apparent conversion. This difference can be rationalized by intramolecular hydrogen bonding in ortho- and para-dihydroxy systems, which stabilizes the neutral form and may hinder full deprotonation under the applied conditions. In contrast, the meta-arrangement in resorcinol prevents such stabilization, facilitating a more effective salt formation. A similar substituent-dependent trend is observed for methylphenols. The relatively high conversion of p-cresol compared to *o*- and *m*-cresol suggests that steric hindrance in the ortho position and electronic effects in the meta position reduce effective interaction with NaOH. Steric shielding of the hydroxyl group in o-cresol likely impedes efficient deprotonation, while inductive effects from the methyl substituent may subtly influence phenoxide stability. More pronounced limitations are observed for methoxy-substituted aromatics. Anisole, 4-methoxyphenol, and syringol show minimal evidence of phenoxide formation. The strong electron-donating resonance effect of methoxy groups increases the electron density in the aromatic ring and can stabilize the neutral phenol through resonance, thereby decreasing the relative acidity of the hydroxyl group. Additionally, steric bulk from multiple methoxy substituents may further hinder access to the base. Guaiacol, however, exhibits moderate phenoxide formation, suggesting that the presence of only one methoxy group does not completely suppress deprotonation but does reduce its efficiency compared with unsubstituted phenols. For alkyl-substituted phenols, 4-propylphenol demonstrates reasonably efficient salt formation, consistent with the moderate electron-donating nature of alkyl groups that do not strongly destabilize the phenoxide. In contrast, eugenol and 2-methoxy-4-propylphenol display very low −ONa signal intensity. In these substrates, the combined steric bulk and electronic donation from both methoxy and allyl/propyl substituents likely reduce phenolic acidity and hinder effective deprotonation. Furthermore, conjugated side chains such as those in eugenol may participate in secondary interactions or side reactions under basic and thermal conditions.

Overall, these findings demonstrate that the classical NaOH-based phenoxide preparation step in the Kolbe−Schmitt protocol is strongly substrate-dependent and therefore not universally applicable to all lignin-derived hydroxybenzenes. While efficient deprotonation is achieved for simpler phenols and selected substituted systems, electron-donating groups, steric hindrance, and intramolecular hydrogen bonding can significantly suppress phenoxide formation in more complex substrates. Consequently, although the method can be successful for certain lignin-derived aromatics, its broader applicability requires further optimization. Future studies should systematically evaluate alternative bases (e.g., KOH, Na_2CO_3, K_2CO_3, and other alkali or alkaline-earth hydroxides and carbonates), as well as the influence of base-to-substrate ratio, temperature, and reaction time, in order to enhance phenoxide formation and enable more efficient downstream carboxylation.

3.2. Direct Carboxylation Reactions of Various Lignin-Derived Aromatics

As discussed in the literature, the Marasse method includes direct carboxylation of the hydroxybenzenes with strong base; as opposed to the Kolbe−Schmitt method, which involves preparation of metal phenoxides (reacting hydroxybenzenes with a strong base) and then subsequent carboxylation.[16] Marasse method is significantly simpler as it includes a single-pot reaction, without the additional steps of two reactions,

https://doi.org/10.1021/acssuschemeng.6c00430
ACS Sustainable Chem. Eng. 2026, 14, 8685−8700

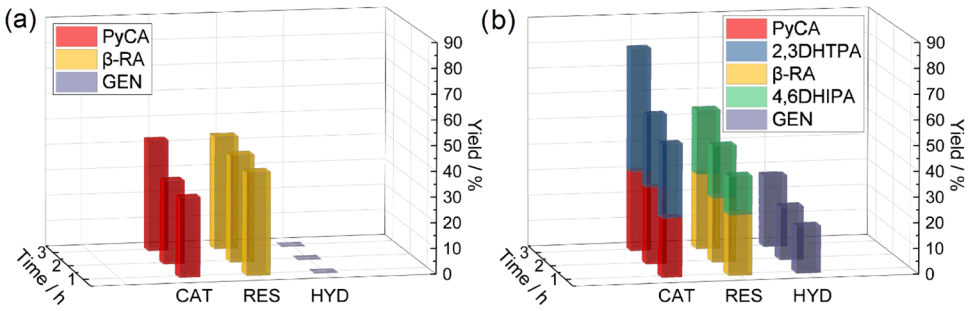

Figure 3. Carboxylation of catechol (CAT), resorcinol (RES), and hydroquinone (HYD) under 150 °C (a) and 200 °C (b) for 1, 2, and 3 h (30 bar of CO_2, 2.5 mmol of dihydroxybenzene, 5.0 mmol of K_2CO_3, 600 rpm).

separation, and drying of the prepared metal phenoxide. From a mechanistic perspective, the key distinction lies in the *in situ* generation of reactive phenoxide species under CO_2 pressure, which may alter both reaction kinetics and selectivity compared to preformed salts. With that in mind, the following section uses the Marasse method, with K_2CO_3 as a base, for screening of carboxylation reactions of various lignin-derived aromatics. The investigated aromatics include hydroxybenzene (phenol), dihydroxybenzenes (catechol, resorcinol, and hydroquinone), methylphenols (*o*-, *m*-, and *p*-cresols), methoxyphenols (anisole, guaiacol, 4-methylphenol, and syringol), and alkylphenols (4-propylphenol, eugenol, and 2-methoxy-4-propylphenol).

3.2.1. Carboxylation of Phenol. Marasse carboxylation of phenol was thoroughly investigated in our previous study,[22] where four strong bases (NaOH, KOH, Na_2CO_3, and K_2CO_3) were tested for both Marasse and Kolbe-Schmitt methods. The results suggested successful Marasse carboxylation of phenol only with K_2CO_3, which is the reason K_2CO_3 was chosen as the base for the Marasse carboxylation screening of other lignin-derived aromatics. In that study, the reactions were carried out in Parr 5000 75 mL reactors, at 200 °C, for 5 h, and the obtained results using K_2CO_3 as a strong base included 27.5% SA, 2.3% 4HBA (4-hydroxybenzoic acid), and 2.1% 4HiPH (4-hydroxyisophthalic acid).[22] This study, as mentioned in the Experimental Section, includes a Parr 2500 reactor system with a 5 mL reactor, and reaction conditions of 2.5 mmol aromatic reactant, 2.5 mmol of K_2CO_3, 30 bar CO_2, and various temperatures and reaction durations. As shown in Figure 2a, at 150 °C, the yield of salicylic acid (SA) increased with reaction time, reaching 47.2%, 53.6%, and 58.6% after 1, 2, and 3 h, respectively. Similarly, an increasing trend was observed for 4HIPh 1.3, 2.4, and 3.1%, while for 4HBA, the obtained yields were decreasing; 6.3, 4.6, 2.1%. These results indicate that under these milder thermal conditions, ortho-carboxylation proceeds progressively and selectively. The gradual rise in 4HIPh with time suggests that secondary carboxylation becomes accessible once sufficient monocarboxylated intermediate accumulates. Interestingly, the decreasing yield of 4HBA over time at 150 °C implies either competitive consumption or thermodynamic preference for the orthoproduct under these conditions. In contrast, at 200 °C (Figure 2b), the reaction profile shifts significantly. SA yields are substantially lower, while para-carboxylated (4HBA) and doubly carboxylated (4HIPh) products become more prominent. SA has shown significantly lower yields than those obtained at 150 °C: 24.0, 25.0, and 30.9%. On the other hand, slightly higher yields were obtained of 4HBA, 16.8, 16.0, and 20.6%, as well as those of 4HIPh, 3.3, 6.7, and 8.2%, after 1, 2, and 3 h, respectively. This temperature dependence suggests that higher thermal energy reduces regioselectivity, potentially by enabling alternative transition states or increasing phenoxide mobility, thereby facilitating para substitution and subsequent secondary carboxylation. Elevated temperature may also promote decarboxylation or product interconversion processes that limit SA accumulation.

In comparison, Mohammad et al.[21] recently reported suspension-based carboxylation of preformed sodium phenolates at 225 °C, achieving high salicylic acid yields under optimized mixing and salt-phase conditions. Their approach relies on isolated sodium phenoxide salts and elevated temperatures to maximize the phenolate reactivity and CO_2 incorporation. In contrast, the present work employs *in situ* carbonate-mediated activation (K_2CO_3) under comparatively milder conditions (150−200 °C, 30 bar of CO_2), allowing systematic evaluation of intrinsic structure−reactivity effects without substrate-specific salt preparation. While suspension-phase sodium systems may afford higher optimized yields, the unified Marasse methodology adopted here provides a consistent benchmarking platform and reveals clear temperature-dependent regioselectivity trends under moderate-pressure conditions.

Overall, the results obtained for phenol clearly demonstrate that both the reactor configuration and reaction temperature critically influence Marasse carboxylation performance. The superior yields achieved in the 5 mL reactor compared to the 75 mL system can be attributed to more efficient stirring and improved gas−liquid−solid contact, which enhance CO_2 accessibility to the in situ generated phenoxide species and thereby promote carboxylation efficiency. For phenol specifically, lower temperatures (150 °C) combined with longer reaction times favor selective ortho-carboxylation, leading to significantly higher salicylic acid (SA) yields. In contrast, increasing the temperature to 200 °C reduces SA selectivity and shifts the product distribution toward para-carboxylated 4-hydroxybenzoic acid (4HBA) and doubly carboxylated 4-hydroxyisophthalic acid (4HIPh). These findings indicate that in the case of phenol, careful control of temperature and mixing conditions is essential for steering regioselectivity and maximizing the formation of the desired ortho-carboxylated product.

3.2.2. Carboxylation of Dihydroxybenzenes. Carboxylation of dihydroxybenzenes was carried out in an identical manner, with a doubling of the amount of K_2CO_3, in order to keep the − OH/K+ ratio the same. This adjustment ensures comparable deprotonation efficiency, which is particularly important for dihydroxy substrates, where competitive mono- and dianionic species may form and influence regioselectivity.

https://doi.org/10.1021/acssuschemeng.6c00430
ACS Sustainable Chem. Eng. 2026, 14, 8685−8700

Scheme S1 in the Supporting Information shows the reaction scheme of catechol (CAT), Scheme S2 shows that of resorcinol (RES), and Scheme S3 shows that of hydroquinone (HYD) carboxylation, including all theoretically possible mono- and dicarboxylated products. The compounds highlighted in color represent the products that were experimentally detected and confirmed under the applied reaction conditions, distinguishing them from other potential but unobserved carboxylation pathways. The three isomeric dihydroxybenzenes exhibit markedly different reactivity patterns, underscoring the strong influence of hydroxyl positioning on both the activation and substitution pathways. As shown in Figure 3a, at 150 °C, catechol and resorcinol each produced a single monocarboxylated product: pyrocatechuic acid (PyCA) and β-resorcylic acid (β-RA), respectively, with steadily increasing yields over time. CAT yielded 31.1, 32.7, and 43.4% of PyCA after 1, 2, and 3 h, respectively, while resorcinol yielded 40.1, 41.8, and 44.1% of β-RA after 1, 2, and 3 h, respectively. The exclusive formation of one regioisomer in both cases suggests that under milder conditions, carboxylation proceeds under kinetic control, favoring substitution at the position activated by the adjacent phenoxide functionality. In catechol, the ortho-dihydroxy arrangement enhances electron density at specific positions via resonance donation, directing CO_2 insertion selectively. Similarly, in resorcinol, the meta relationship between hydroxyl groups defines a distinct activation pattern that favors β-RA formation. Hydroquinone, in contrast, showed no detectable carboxylation at 150 °C. The para arrangement of hydroxyl groups may stabilize the dianionic form differently and reduce the effective nucleophilicity at reactive positions under these milder conditions. Only at 200 °C (Figure 3b) does hydroquinone undergo carboxylation to yield gentisic acid (GEN), indicating that higher thermal energy is required to overcome its lower intrinsic reactivity. This behavior highlights how subtle differences in the substitution pattern significantly affect the balance between deprotonation, CO_2 insertion, and competing stabilization effects.

Increasing the temperature to 200 °C not only alters the reactivity but also shifts the product distribution toward double carboxylation for catechol and resorcinol. In both systems, monocarboxylated intermediates remain substantial, yet significant formation of dicarboxylated products (2,3-dihydroxyterephthalic acid (2,3DHTPA) from catechol and 4,6-dihydroxyisophthalic acid (4,6DHIPA) from resorcinol) is observed. After 1, 2, and 3 h of carboxylation of CAT at 200 °C, 23.1, 30.0, and 31.1% of PyCA were obtained, respectively, while 28.9, 28.5, and 28.4% of 2,3DHTPA were obtained, respectively. After 1, 2, and 3 h of RES carboxylation at 200 °C, 23.6, 25.0, and 29.5% of β-RA were obtained, respectively, while 15.0, 20.6, and 29.5% of 4,6DHIPA were obtained, respectively. This suggests that once the first carboxyl group is introduced, the remaining phenolic functionality can undergo a second deprotonation−carboxylation sequence under more compelling conditions. The comparable yields of mono- and dicarboxylated products at prolonged reaction times indicate that secondary carboxylation becomes competitive rather than merely consecutive, reflecting increased activation of the ring after initial substitution.

Comparison with literature reveals that while monocarboxylation of resorcinol and catechol has been reported under various thermal, pressurized, and even biocatalytic conditions, the formation of double-carboxylated products is rarely observed. Most prior studies focus on optimizing β-resorcylic or ortho-hydroxy acid formation, with yields strongly dependent on pressure, temperature, and reactor design. Shanthi et al.[26] have shown that resorcinol carboxylation with KOH under ultrasonication can produce β-RA between 30 and 65%, depending on the sonication amplitude used. Krtschil et al.[27] have shown that the 32% β-RA yield (9 g h^{-1}) obtained in the capillary reactor can be scaled up to a continuously operated pilot reactor to increase the productivity to 520 g h^{-1}, with γ-RA detectable in trace amounts. Barbarossa et al.[28] have studied resorcinol carboxylation (80−120 °C) in aqueous KOH, in terms of CO_2 loading capacity ($CO_{2(absorbed)}$/$resorcinol_{(starting)}$ % on a molar scale), and have obtained between 15 and 37% loading capacity at 30 bar CO_2 pressure (increasing capacity with increasing temperature, reaction time, and pressure). Baine et al.[16] obtained 65% β-RA under 125 °C, 8 h, and 83−138 bar, from batch resorcinol carboxylation. They also used the same pressure for catechol and hydroquinone carboxylation (225 °C, 4 h, and 200 °C, 8 h, respectively) to obtain 72 and 49% of the respective ortho-hydroxy acids. The literature mostly focuses on biocatalytic carboxylation of catechol, while chemical catechol carboxylation remains poorly investigated.[29,30] Hessel et al.[31] have used the aqueous Kolbe-Schmitt method for carboxylation of resorcinol and hydroquinone in a capillary reactor; however, while using $KHCO_3$ as a carboxylating agent, instead of gaseous CO_2, and have obtained less than 1% of respective acids. Plasch et al.[32] have shown that resorcinol carboxylation is also possible via biocatalytic methods, using 2,3-dihydroxybenzoic acid decarboxylase from *Aspergillus oryzae* or salicylic acid decarboxylase from *Trichosporon moniliiforme*, 30 °C and 30 bar CO_2 for 24 h, to obtain to 68% resorcinol conversion (not mentioning yields and selectivity). Overall, none of these studies have reported the formation of any double-carboxylated products (nor any other report on resorcinol, catechol, or hydroquinone carboxylation), which leaves our study being the first to report chemical formation of 4,6-dihydroxyisophthalic acid, a double-carboxylated resorcinol. Double-carboxylated catechol (4,5-dihydroxyisophthalic acid, 4,5DHTPA) has previously been reported only by Mohammad et al.[21] under suspension-based carboxylation of sodium catecholate at elevated temperature. In our study, double carboxylation reaches up to 28.9% 2,3DHTPA, representing a clear improvement in yield, compared to their 19.7%. The substitution of Na^+ with K^+ in a carbonate-mediated activation approach may modify phenoxide coordination and reactivity, thereby enhancing the efficiency of sequential CO_2 incorporation. Generally, the comparison highlights that both cation identity and the reaction system employed (suspension-based preformed phenolates versus *in situ* carbonate-mediated activation) play a decisive role in enabling higher levels of double carboxylation within a unified experimental framework.

Overall, the reactivity trends among catechol, resorcinol, and hydroquinone highlight how hydroxyl positioning governs both activation and selectivity in direct CO_2 carboxylation. Lower temperatures favor kinetically controlled monocarboxylation, whereas elevated temperatures promote further ring activation and enable double carboxylation. These findings expand the scope of chemical carboxylation of lignin-derived dihydroxy aromatics and reveal temperature as a key parameter for steering between selective monofunctionalization and higher degrees of substitution.

https://doi.org/10.1021/acssuschemeng.6c00430
ACS Sustainable Chem. Eng. 2026, 14, 8685−8700

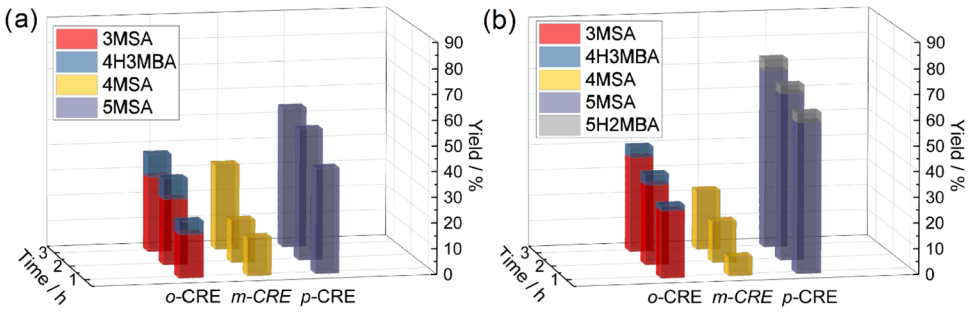

Figure 4. Carboxylation of *o*-cresol (*o*-CRE), *m*-cresol (*m*-CRE), and *p*-cresol (*p*-CRE) under 150 °C (a) and 200 °C (b) for 1, 2, and 3 h (30 bar of CO_2, 2.5 mmol of methylphenol, 2.5 mmol of K_2CO_3, 600 rpm).

3.2.3. Carboxylation of Methylphenols. Carboxylation of methylphenols was carried out in a manner identical with that of the phenol carboxylation, with the same $-OH/K^+$ ratio. Figures S4–S6 in the Supporting Information show reaction schemes of *o*-cresol (*o*-CRE), *m*-cresol (*m*-CRE), and *p*-cresol (*p*-CRE) carboxylation, respectively, with all the potential mono- and dicarboxylated products, while colored compounds were the only ones obtained in this study. The presence of the methyl group introduces both electronic (electron-donating via hyperconjugation) and steric effects, which strongly influence the regioselectivity in CO_2 insertion. Consequently, the three cresol isomers display distinct reactivity patterns depending on substitution geometry and reaction temperature.

As shown in Figure 4a, at 150 °C, the carboxylation of *o*-CRE yielded two products: 3-methylsalicylic acid (3MSA) and 4-hydroxy-3-methylbenzoic acid (4H3MBA). The yield of 3MSA increased with reaction time, reaching 17.0%, 25.5%, and 29.2% after 1, 2, and 3 h, respectively. The dominance of 3MSA indicates preferential ortho-carboxylation relative to the hydroxyl group, consistent with classical Kolbe–Schmitt orientation. However, the modest formation of 4H3MBA suggests that steric hindrance imposed by the adjacent methyl group partially redirects substitution toward the para position. In contrast, carboxylation of *m*-CRE and *p*-CRE yielded a single detectable product at 150 °C. For *m*-CRE, 4-methylsalicylic acid (4MSA) was obtained in 15.0, 16.5, and 33.2% after 1, 2, and 3 h, respectively, while for *p*-CRE, 5-methylsalicylic acid (5MSA) was obtained in significantly higher yields of 41.0, 51.3, and 54.8% after 1, 2, and 3 h, respectively. The high selectivity observed for *p*-CRE can be attributed to the absence of steric congestion near the reactive ortho position, enabling efficient intramolecular stabilization of the transition state, leading to salicylic-type products. The strong time-dependent increase in 5MSA further suggests that under these conditions, carboxylation proceeds steadily without substantial competitive degradation.

Raising the temperature to 200 °C (Figure 4b) modifies both the activity and selectivity. For *o*-CRE, 3MSA yields increased to 26.1, 31.1, and 36.9% after 1, 2, and 3 h, respectively, while 4H3MBA was no longer detected in significant amounts. The disappearance of 4H3MBA at elevated temperatures likely reflects its lower thermal stability; para-hydroxybenzoic-type structures are more susceptible to decarboxylation under harsh conditions. This interpretation aligns with thermogravimetric analyses and high-temperature studies reported in the literature, where 4H3MBA was shown to decompose upon heating.[21,33] Notably, no double-carboxylated *o*-cresol products were detected under these conditions, in contrast to reports at 225 °C in sodium cresolate systems. For *m*-CRE, increasing the temperature to 200 °C led to reduced overall 4MSA formation, with yields of 7.4, 16.0, and 23.1% after 1, 2, and 3 h, respectively. This decrease relative to 150 °C suggests that a higher temperature may promote either competing side reactions or partial decarboxylation, indicating that *m*-cresol carboxylation is less thermally robust. In contrast, *p*-CRE exhibits enhanced performance at 200 °C. The yields of 5MSA increased to 58.8, 65.2, and 69.4% after 1, 2, and 3 h, respectively, and an additional product, 5-hydroxy-2-methylbenzoic acid (5H2MBA), was detected in 3.7, 3.4, and 4.4%, respectively. The simultaneous increase of both monocarboxylated products indicates that p-cresol-derived intermediates are comparatively stable at elevated temperature and that higher thermal energy facilitates secondary rearrangements or alternative substitution pathways without significant decomposition. The thermal resilience of these products suggests that under even more compelling conditions, further carboxylation toward double-substituted derivatives such as 3-hydroxy-6-methylphthalic acid or 2-hydroxy-5-methylterephthalic acid may become feasible.

Comparison with the literature reveals that substantially higher yields have been achieved under supercritical CO_2 conditions and elevated temperatures, highlighting the importance of the CO_2 density and enhanced mass transfer for improved conversions. In the study by Baine et al.,[16] they were able to obtain significantly higher yields when conducting *o*-, *m*-, and *p*-cresol carboxylation under supercritical CO_2 conditions (83–138 bar CO_2). After 4 h, under 175 °C, they obtained 70, 85, and 85% of corresponding o-hydroxy acids, from *o*-, *m*-, and *p*-cresol, respectively. Cameron et al.[17] also used SC CO_2 to investigate various reaction conditions on *p*-CRE carboxylation and also obtained up to 85% 5MSA. Mohammad et al.[21] reported successful carboxylation of toluene suspension-based sodium cresolate (2-CrONa), under 225 °C, and obtained up to 89.2% 3MSA, 12.4% 4H3MBA, and 4.4% double-carboxylated 4-hydroxy-5-methyl-isophthalic acid (4H5MIPA). When comparing, our results show a lack of 4H3MBA at elevated temperatures (200 °C) and no detection of double-carboxylated *o*-cresol. This could be explained by the lower thermal stability of the 4H3MBA, which, upon exposure to higher temperatures, deteriorates due to decarboxylation. On the other hand, the results show that *p*-CRE and its monocarboxylated products (5MSA and 5H2MBA) are more stable at higher temperatures, and their increasing yields were obtained with increasing temperature. This would suggest that upon exposure to higher temperatures or longer reaction times, they could be converted to double-carboxylated products, 3-hydroxy-6-methylphthalic acid

https://doi.org/10.1021/acssuschemeng.6c00430
ACS Sustainable Chem. Eng. 2026, 14, 8685–8700

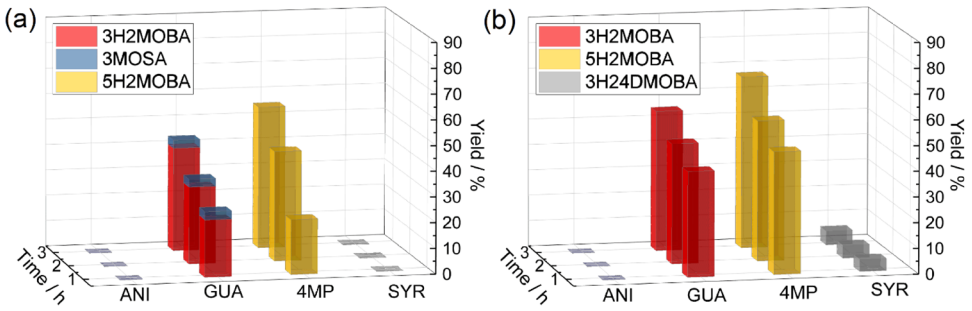

Figure 5. Carboxylation of anisole (ANI), guaiacol (GUA), 4-methoxyphenol (4MP), and syringol (SYR) under 150 °C (a) and 200 °C (b) for 1, 2, and 3 h (30 bar of CO_2, 2.5 mmol of methoxyphenol, 2.5 mmol of K_2CO_3, 600 rpm).

(3H6MPA) or 2-hydroxy-5-methylterephthalic acid (2H5MTPA).

Overall, methyl substitution exerts a pronounced steric and electronic influence on the CO_2 carboxylation. Para-cresol shows the highest intrinsic reactivity and thermal stability, o-cresol displays temperature-sensitive selectivity due to steric effects and product instability, and m-cresol appears most sensitive to elevated temperatures. These trends demonstrate how subtle positional changes in lignin-derived aromatics significantly affect both the regioselectivity and thermal robustness in direct carbonate-mediated CO_2 carboxylation.

3.2.4. Carboxylation of Methoxyphenols. Carboxylation of methoxyphenols was carried out in a manner identical with that of the phenol carboxylation, keeping the same −OH/K^+ ratio, in order to directly assess the influence of methoxy substitution on CO_2 incorporation. Figures S7−S10 in the Supporting Information show reaction schemes of anisole (ANI), guaiacol (GUA), 4-methoxyphenol (4MP), and syringol (SYR) carboxylation, respectively, with all the potential mono- and dicarboxylated products, while colored compounds were the only ones obtained in this study. Methoxy groups are strongly electron-donating via resonance (+M effect), which increases electron density of the aromatic ring but simultaneously decreases the acidity of the phenolic −OH group. As a result, deprotonation efficiency and subsequent phenoxide reactivity are expected to be more sensitive to temperature compared to unsubstituted phenols.

At 150 °C (Figure 5a), anisole (ANI) and syringol (SYR) did not yield any detectable carboxylated products after 1, 2, or 3 h, indicating that either deprotonation (in the case of SYR) or electrophilic CO_2 insertion was insufficient under these conditions. The complete lack of reactivity for ANI clearly confirms the essential role of the phenolic −OH group in Kolbe−Schmitt-type carboxylation: without the ability to form a phenoxide intermediate, CO_2 activation and directed substitution do not occur. In contrast, guaiacol (GUA) and 4-methoxyphenol (4MP), each containing one phenolic −OH group, showed measurable reactivity at 150 °C. For GUA, 3-hydroxy-2-methoxybenzoic acid (3H2MOBA) was obtained in 22.3, 30.0, and 40.3% after 1, 2, and 3 h, respectively, while 3-methoxysalicylic acid (3MOSA) was consistently formed in 3.2, 3.1, and 3.2%, respectively. The dominance of 3H2MOBA suggests preferential carboxylation at the position activated by both hydroxyl and methoxy substituents. The relatively constant and low formation of 3MOSA indicates a minor competing regioisomer pathway likely disfavored sterically or electronically. For 4MP at 150 °C, 5-hydroxy-2-methoxybenzoic acid (5H2MOBA) was obtained in 21.3, 42.9, and 55.4% after 1, 2, and 3 h, respectively. The pronounced increase with time and the absence of competing products indicate strong regioselective control and progressive conversion under these conditions. The para arrangement of methoxy and hydroxy groups likely minimizes steric hindrance and enables efficient stabilization of the ortho-carboxylated transition state.

Upon increasing the temperature to 200 °C (Figure 5b), the reactivity increased significantly for substrates containing phenolic −OH groups. Anisole remained completely unreactive, further reinforcing that phenoxide formation is a prerequisite for carboxylation. For GUA, yields of 3H2MOBA increased to 41.1, 54.9, and 54.8% after 1, 2, and 3 h, respectively, demonstrating that elevated temperature enhances the CO_2 insertion efficiency, likely by overcoming reduced phenolic acidity caused by the methoxy substituent. Similarly, 4MP exhibited increased formation of 5H2MOBA at 47.8, 54.9, and 67.3% after 1, 2, and 3 h, respectively. The strong temperature dependence indicates that methoxy-substituted systems require additional thermal activation to achieve high conversion, consistent with their reduced acidity relative to phenol or cresols. Syringol, bearing two methoxy groups, displayed the lowest reactivity. Only at 200 °C was 3-hydroxy-2,4-dimethoxybenzoic acid (3H24DMOBA) detected, in 4.8, 5.1, and 5.5% after 1, 2, and 3 h, respectively. The minimal conversion reflects the combined steric hindrance and strong electron-donating effects of two methoxy substituents, which substantially decrease effective deprotonation and alter ring activation patterns. The data therefore suggest that increasingly substituted methoxyphenols require progressively higher thermal input to achieve measurable carboxylation.

Comparison with the literature supports these observations. Previous studies under supercritical CO_2 conditions (73−137 bar) reported 47% of 3H2MOBA from guaiacol at 200 °C and 4 h, values comparable to or lower than those obtained here at significantly lower CO_2 pressure (30 bar).[16] However, substantially higher yields (90%) were reported for 4MP under supercritical conditions, highlighting the beneficial effect of increased CO_2 density and mass transfer. Similarly, sodium guaiacolate systems at 225 °C have produced up to 86.1% monocarboxylated guaiacol (not specifying which one), confirming that more forcing conditions enhance the reactivity of methoxy-substituted substrates.[21]

Overall, the results demonstrate that methoxy substitution reduces the intrinsic reactivity toward CO_2 carboxylation by lowering phenolic acidity and introducing steric constraints. Higher temperatures are therefore required to achieve substantial conversion, particularly for highly substituted systems such as syringol. Most importantly, the complete lack of anisole reactivity unequivocally confirms that the presence of a phenolic −OH group—and thus the ability to

https://doi.org/10.1021/acssuschemeng.6c00430
ACS Sustainable Chem. Eng. 2026, 14, 8685−8700

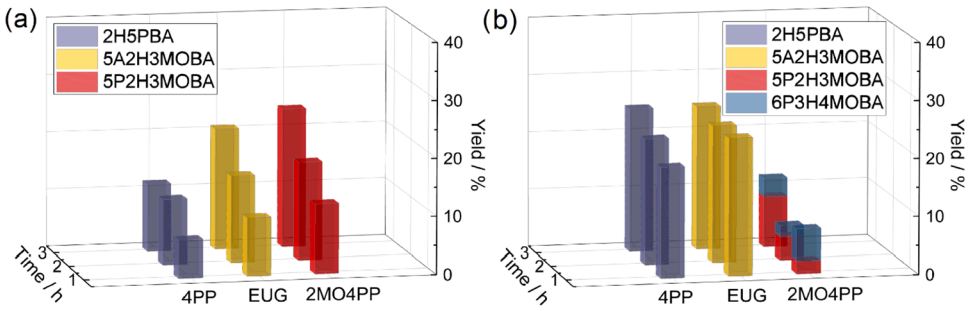

Figure 6. Carboxylation of 4-propylphenol (4PP), eugenol (EUG), and 2-methoxy-4-propylphenol (2MO4PP) under 150 °C (a) and 200 °C (b) for 1, 2, and 3 h (30 bar of CO_2, 2.5 mmol of alkylphenol, 2.5 mmol of K_2CO_3, 600 rpm).

generate a phenoxide intermediate—is indispensable for successful Kolbe−Schmitt-type carboxylation.

3.2.5. Carboxylation of Alkylphenols. Carboxylation of alkylphenols was carried out in an identical manner as for the phenol and other monohydroxylated substrates, maintaining the same $-OH/K^+$ ratio to ensure comparable phenoxide formation. In these systems, the presence of alkyl and allyl substituents introduces additional steric bulk and electron-donating effects, both of which can influence regioselectivity and the stability of carboxylated intermediates. Compared to simpler phenols and cresols, these lignin-derived alkylphenols represent structurally more complex substrates and therefore provide insight into how side-chain substitution affects Kolbe−Schmitt-type CO_2 incorporation. Figures S11−S13 in the Supporting Information show reaction schemes of 4-propylphenol (4PP), eugenol (EUG), and 2-methoxy-4-propylphenol (2MO4PP) carboxylation, respectively, with all the potential mono- and dicarboxylated products, while colored compounds were the only ones obtained in this study.

At 150 °C (Figure 6a), all three substrates yielded a single detectable monocarboxylated product, suggesting that under milder conditions, the reaction proceeds with high regioselectivity but limited overall conversion. Carboxylation of 4PP afforded 2-hydroxy-5-propylbenzoic acid (2H5PBA) in 6.6, 11.3, and 11.7% after 1, 2, and 3 h, respectively. The relatively modest yields indicate that the propyl substituent may partially hinder access to the ortho position or reduce effective phenoxide reactivity compared to that of phenol or cresols. Eugenol (EUG), which contains both an allyl side chain and a methoxy substituent, produced 5-allyl-2-hydroxy-3-methoxybenzoic acid (5A2H3MOBA) in 10.1, 15.1, and 21.0% after 1, 2, and 3 h, respectively. The gradual increase with time suggests steady formation of the monocarboxylated product, while the absence of competing regioisomers implies strong directing effects imposed by the combined hydroxyl and methoxy substituents. Similarly, carboxylation of 2MO4PP produced 5-propyl-2-hydroxy-3-methoxybenzoic acid (5P2H3MOBA) in 12.0, 17.0, and 24.1% after 1, 2, and 3 h, respectively. The slightly higher yields relative to 4PP at 150 °C may reflect the additional activating influence of the methoxy group, which enhances the ring electron density and stabilizes the carboxylation transition state.

Increasing the temperature to 200 °C (Figure 6b) significantly enhanced the reactivity for 4PP and EUG while maintaining the formation of the same primary products. For 4PP, yields of 2H5PBA increased to 19.1, 21.8, and 24.9% after 1, 2, and 3 h, respectively, demonstrating a clear positive temperature effect, likely associated with improved CO_2 insertion kinetics and increased phenoxide reactivity. For EUG, 5A2H3MOBA was obtained in 23.8, 23.7, and 24.9% after 1, 2, and 3 h, respectively. The relatively stable yields between 1 and 2 h suggest that equilibrium or competing thermal processes may limit further accumulation, while the slight increase at 3 h indicates continued, though slower, conversion. The structural complexity of eugenol, including its allyl side chain, may introduce competing thermal pathways at elevated temperatures, potentially restricting further increases in the yield. In contrast, 2MO4PP exhibited a notable change in product distribution at 200 °C. The yield of 5P2H3MOBA decreased substantially to 2.2, 4.0, and 8.7% after 1, 2, and 3 h, respectively, and an additional regioisomer, 6-propyl-3-hydroxy-4-methoxybenzoic acid (6P3H4MOBA), was formed in 5.5, 2.0, and 3.3%, respectively. This shift suggests that at higher temperatures, competing pathways such as isomerization, partial decarboxylation, or altered regioselective control become significant. The combined steric effects of both propyl and methoxy substituents likely destabilize the initially favored product and permit alternative substitution patterns under more forcing conditions. The overall lower yields at 200 °C compared to 150 °C for 2MO4PP indicate the reduced thermal robustness of its carboxylated derivatives.

Literature reports on the chemical carboxylation of lignin-derived alkylphenols are scarce, particularly for 4-propylphenol and 2-methoxy-4-propylphenol. Eugenol has been more extensively studied in biocatalytic systems, where bicarbonate and engineered *Escherichia coli* whole cells have enabled the selective formation of corresponding ortho-hydroxybenzoates under ambient CO_2 pressure.[34] Additionally, eugenol has been utilized in CO_2-based copolymerization routes via epoxide intermediates.[35] However, the direct Kolbe−Schmitt-type carboxylation of these alkylphenols has not previously been systematically reported.

Overall, the results demonstrate that alkyl substitution generally lowers the reactivity compared to simpler phenols, likely due to increased steric hindrance and modified electronic distribution. Temperature enhances the carboxylation efficiency for 4PP and EUG, while 2MO4PP exhibits decreased selectivity and product stability at elevated temperature. Importantly, this study represents the first systematic report of direct Kolbe−Schmitt-type carboxylation of lignin-derived alkylphenols such as 4-propylphenol, eugenol, and 2-methoxy-4-propylphenol, thereby extending the scope of CO_2 utilization chemistry toward more structurally complex biobased aromatics.

A comparative evaluation of all investigated substrate classes, including phenol, dihydroxybenzenes, methylphenols, methoxyphenols, and alkylphenols (tabulated and comprehensively reported in Table S1 in the Supporting Information), reveals

https://doi.org/10.1021/acssuschemeng.6c00430
ACS Sustainable Chem. Eng. 2026, 14, 8685−8700

Table 1. Phosphorus Nuclear Magnetic Resonance (^{31}P NMR) and Size Exclusion Chromatography (SEC) Results of Original Lignin and the Products of Reactions under 150−200 °C and 1−3 h

			^{31}P NMR						SEC		
entry	temp./°C	time/h	aliphatic −OH	syringyl −OH	guaiacyl −OH	phenolic −OH	total −OH	−COOH	M_w	M_n	$Đ$
1	original lignin	2.99	0.84	0.87	2.13	5.20	0.02	3160	908	3.48	
2	150	1	2.62	0.75	0.77	1.93	4.63	0.09	4335	1093	3.96
3		2	2.57	0.76	0.78	1.93	4.58	0.11	9397	1631	5.76
4		3	1.96	0.59	0.59	1.50	3.52	0.06	20,800	2057	10.01
5	200	1	1.20	0.34	0.35	0.89	2.14	0.05	N/A		
6		2	0.35	0.20	0.16	0.48	0.86	0.03			
7		3	0.29	0.21	0.16	0.50	0.82	0.03			

that carbonate-mediated, Kolbe−Schmitt-type carboxylation under pressurized CO_2 is strongly governed by phenolic acidity, substitution pattern, steric effects, and temperature. The presence of a free phenolic −OH group is indispensable, as demonstrated by the complete lack of reactivity of anisole, confirming that *in situ* phenoxide formation is a prerequisite for the CO_2 insertion. Regioselectivity is highly substrate-dependent: phenol exhibits temperature-controlled selectivity, with lower temperatures favoring ortho-carboxylation and higher temperatures promoting para- and decarboxylation. Catechol and resorcinol readily undergo monocarboxylation at 150 °C and enable sequential double carboxylation at 200 °C, whereas hydroquinone requires elevated temperature for activation. Among methylphenols, *p*-cresol shows the highest intrinsic reactivity and thermal stability, while *o*- and *m*-cresol are more sensitive to steric and thermal effects. Methoxyphenols require higher activation energy due to reduced phenolic acidity, with guaiacol and 4-methoxyphenol responding positively to increased temperature and syringol remaining weakly reactive. Alkylphenols generally display lower overall conversion, reflecting increased steric hindrance and a modified electronic distribution. Temperature acts as a selectivity switch. At 150 °C, the reaction typically favors kinetically controlled monocarboxylation. In contrast, 200 °C enhances conversion, broadens substitution patterns, and, in some systems, enables secondary carboxylation, although occasionally at the expense of product stability. Overall, the results demonstrate that successful CO_2 incorporation into lignin-derived aromatics requires careful balancing of electronic activation, steric accessibility, and thermal input, thereby systematically extending Kolbe−Schmitt-type chemistry to structurally diverse biobased substrates.

3.3. Direct Carboxylation of Pure Lignin

As the previous investigations covered direct carboxylation reaction between gaseous CO_2 and various single lignin-derived hydroxybenzenes, this section will investigate the possibility to bypass the depolymerization, cracking, and isolation of lignin-derived aromatics. With this, a significant amount of work would be omitted in obtaining pure and isolated hydroxybenzenes. Currently, four principal industrial techniques are employed for lignin extraction: sulfite, soda, Kraft, and organosolv.[11] Each approach aims to isolate and chemically break down the lignin macromolecule into smaller fragments that can dissolve in the medium. The resulting lignin fractions vary in molecular weight due to differences in depolymerization during separation as well as condensation reactions among the degraded intermediates. In the environmentally friendly organosolv method, a mixture of water and an organic solvent combined with organic or mineral acids promotes hydrolysis. During pretreatment, bonds between lignin and carbohydrates, as well as α-O-4 linkages, are primarily cleaved to release lignin from the lignocellulosic biomass. Under relatively mild operating conditions, organosolv is particularly effective in maintaining lignin's native structure, which contains a high proportion of β-O-4 ether bonds.[36]

After obtaining the beech sawdust from the Slovenian wood-processing company, the organosolv isolation method[37] was used to obtain pure lignin. The isolated beech organosolv lignin was subsequently used as the substrate for all of the direct carboxylation reactions discussed in this section. Table 1 shows the amounts of different −OH groups (aliphatic, syringyl, guaiacyl, and phenolic) as well as the carboxylic −COOH groups, obtained by ^{31}P NMR. Size exclusion chromatography (SEC) was used to obtain the average molecular mass (M_w), number-average (M_n), and dispersity of the isolated lignin ($Đ$), all shown in Table 1, and visually presented in Figure 7. The original lignin contains 5.20 mmol/g of total −OH groups, most of which come from aliphatic (2.99) and phenolic (2.19) origin. Carboxylic groups are present in the amount of 0.02 mmol/g. The average molecular weight of isolated lignin is 3160 Da, with the average number of monomer units being 908, thus having a dispersity ratio of 3.48.

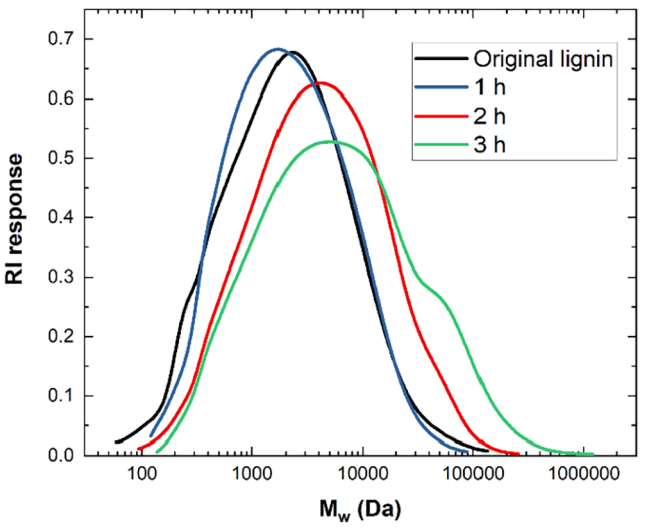

Figure 7. Size exclusion chromatography (SEC) results of pure lignin (black) and results obtained after 1 (blue), 2 (green), and 3 h (red) of lignin carboxylation under 150 °C.

After thorough characterization of pure lignin, the lignin was used for direct carboxylation reactions. Figure 8 presents the

https://doi.org/10.1021/acssuschemeng.6c00430
ACS Sustainable Chem. Eng. 2026, 14, 8685−8700

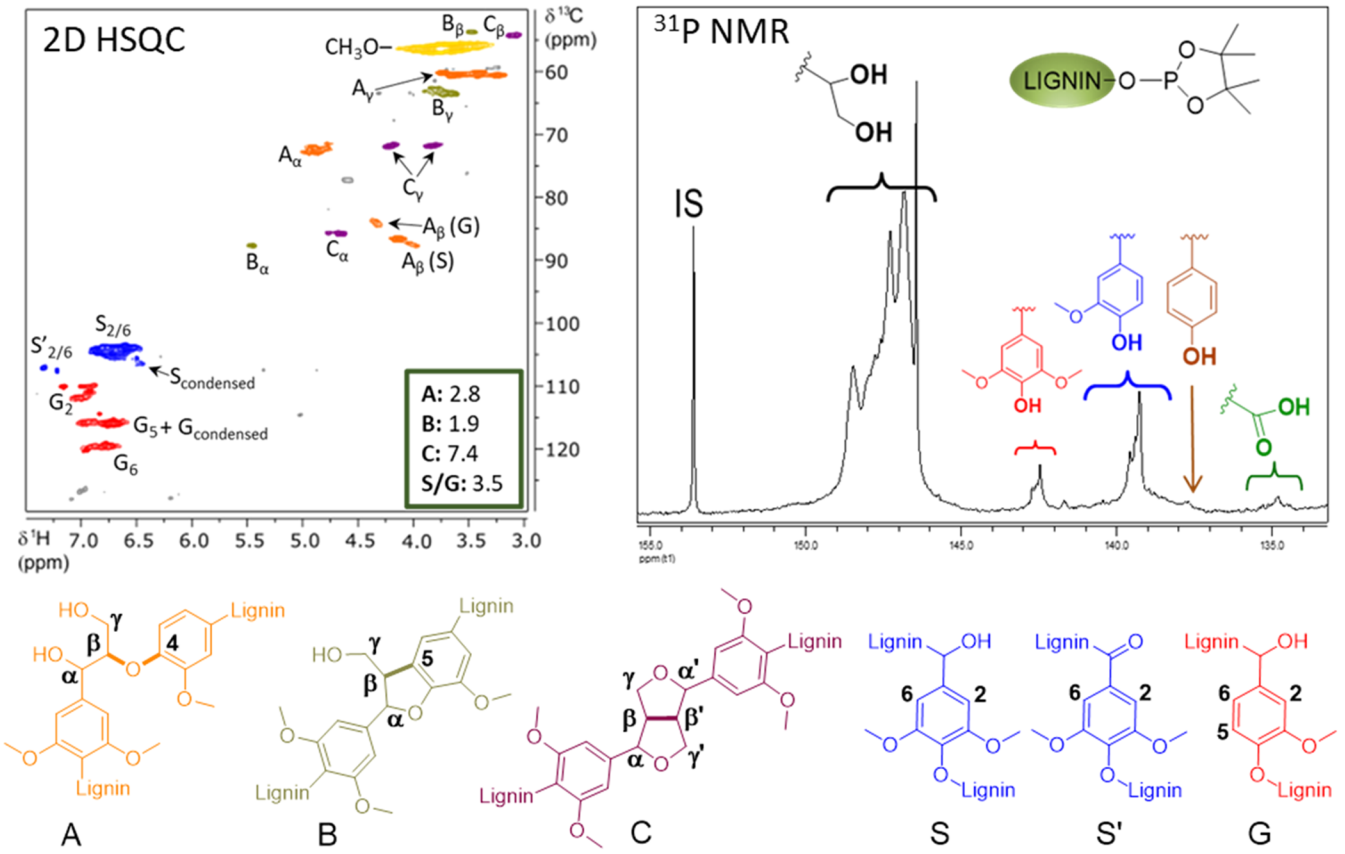

Figure 8. Quantitative ^{31}P NMR and 2D HSQC spectra of beech lignin and major structures of lignin: A, (β-O-4) β-aryl-ether units; B, (β-5) phenylcoumaran structures; C, (β-β) resinol structures; S, syringyl units; S′, oxidized syringyl units; G, guaiacyl units.

structural characterization of the starting beech lignin by quantitative ^{31}P NMR and 2D HSQC spectroscopy. The HSQC spectrum confirms the presence of the dominant β-O-4, β-5, and β-β interunit linkages as well as syringyl (S) and guaiacyl (G) aromatic units typical for hardwood lignin. Quantitative ^{31}P NMR further establishes the distribution of aliphatic and phenolic hydroxyl groups, providing a structural baseline for evaluating subsequent carboxylation-induced modifications. Considering the amount of total −OH groups (5.20 mmol/g), the ratio of the −OH groups to the available potassium ions was kept identical (1:2) as in all the previous carboxylation reactions of pure lignin-derived model compounds. The reaction between 0.3 g of isolated lignin and 0.27 g of K_2CO_3 was also conducted at two temperatures (150 and 200 °C), and three time intervals (1, 2, and 3 h), under 30 bar of gaseous CO_2. The obtained products were also characterized with ^{31}P NMR and SEC, and are tabulated in Table 1. The products obtained under 200 °C and all three reaction durations (entries 5, 6, and 7) were impossible to dissolve in the dedicated liquid media (pyridine) even after extended heating and sonication cycles. The insolubility of products obtained at 200 °C is more plausibly attributed to extensive thermally induced condensation and repolymerization reactions rather than simple physical agglomeration. Under elevated temperatures, lignin undergoes cleavage of β-O-4 linkages followed by rapid recombination of reactive intermediates via C−C bond formation, a behavior well documented during lignin pyrolysis under inert atmospheres such as N_2.[38,39] These harsh conditions would primarily distort the molecule, deteriorate its physicochemical structure, and consequently disallow its successful carboxylation. Results obtained from ^{31}P NMR confirm this, as seen by obtaining significantly lower amounts of all the −OH and −COOH groups than present in the original lignin.

On the other hand, products obtained from reactions carried out at 150 °C (Entries 2, 3, and 4) were readily dissolved in pyridine, allowing accurate characterization. After 1 h, the −COOH content increased from 0.02 to 0.09 mmol g^{-1}, indicating that the incorporation of CO_2 into the lignin structure does occur under these conditions. Extending the reaction time to 2 h further increased the −COOH content to 0.11 mmol g^{-1}. However, these changes must be interpreted alongside simultaneous structural transformations. The total −OH content decreased from 5.20 mmol g^{-1} in the original lignin to 4.63 mmol g^{-1} after 1 h and 4.58 mmol g^{-1} after 2 h, while the weight-average molecular weight (Mw) increased from 3160 to 4335 and 9397 Da, respectively, with a corresponding increase in dispersity from 3.48 to 3.96 and 5.76. These trends indicate that, in parallel with CO_2 incorporation, condensation, and repolymerization reactions are already significant. After 3 h, this behavior becomes dominant, as evidenced by a sharp increase in Mw to 20,800 Da and a decrease in total −OH groups to 3.52 mmol g^{-1}, accompanied by a reduction in −COOH content to 0.06 mmol g^{-1}. Therefore, although carboxylation is clearly detectable, it represents only a minor contribution to the overall transformation of lignin, which is primarily governed by thermally induced condensation processes.

The evolution of the molecular weight further supports the dominance of condensation processes. While incorporation of

https://doi.org/10.1021/acssuschemeng.6c00430
ACS Sustainable Chem. Eng. 2026, 14, 8685−8700

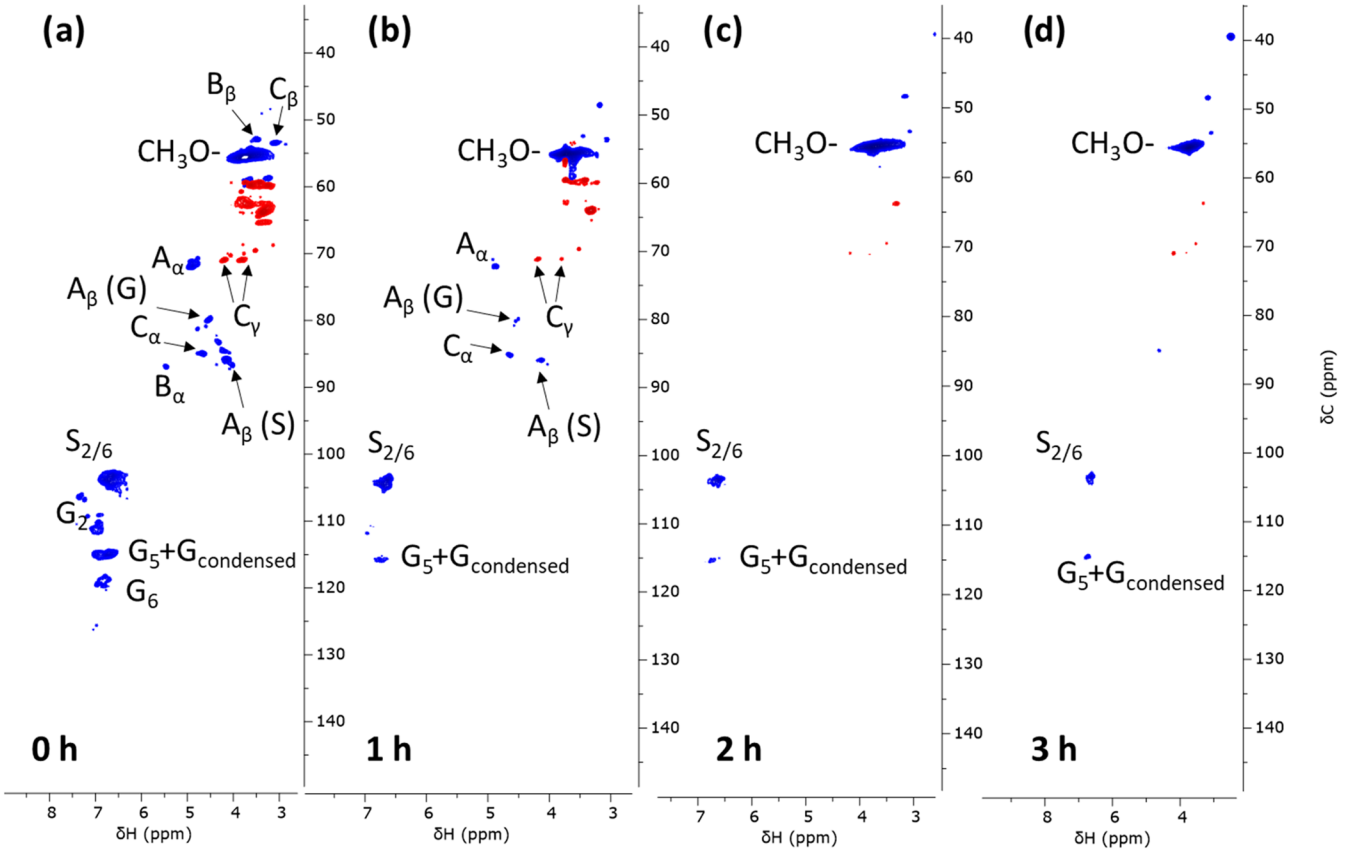

Figure 9. 2D HSQC NMR spectra of reference lignin (a) and reaction products: (b) after 1 h, (c) after 2 h, and (d) after 3 h.

−COOH groups contributes marginally to molecular weight changes, the substantial increase in Mw from 3160 to 4335 Da, 9397 Da, and ultimately 20800 Da indicates that intermolecular coupling reactions are the primary driving force. This behavior is consistent with the formation of reactive intermediates following *β*-O-4 bond cleavage, which undergo recombination through C−C bond formation. Consequently, the observed increase in molecular weight reflects the chemical restructuring and cross-linking of lignin rather than effective functionalization through carboxylation. Reactive phenoxy and quinone methide intermediates generated during thermal treatment can undergo C−C coupling, leading to highly cross-linked macromolecular structures.[40] This mechanistic pathway closely resembles the lignin behavior observed during thermal processing, where depolymerization is rapidly followed by repolymerization and char-like network formation.

The thermogravimetric study of lignin pyrolysis carried out by Li et al.[41] supports our claims and results. They have shown that the agglomeration and decomposition of lignin start at temperatures slightly below 200 °C. However, an additional study has shown that agglomeration of lignin can be somewhat controlled by the addition of various alkaline additives.[42] Monoacidic bases (NaOH, KOH), diacidic bases ($Ca(OH)_2$, $Mg(OH)_2$), and triacidic bases ($Al(OH)_3$) have been shown to be effective; however, no studies have investigated the effect of alkali carbonates on the agglomeration, condensation, and degradation of lignin.

Detailed insight into the structural evolution of lignin during treatment was obtained using 2D HSQC, quantitative ^{31}P NMR, and SEC analyses, as shown in Figure 9. A gradual reduction in the $S_{2/6}$ cross-signal at δC 102.7−104.7 and δH 6.8−6.5 ppm intensity was observed over time, most likely due to the progressive incorporation of −COOH functionalities into the syringyl unit (S). Simultaneously, the earliest detectable structural modification was the appearance of primary carboxylation at the G_6 position, followed by the subsequent introduction of −COOH groups at the G_2 position in the guaiacyl unit (G). As the reaction proceeded, all interunit linkages were cleaved, leaving only trace amounts of *β*-*β* structures, confirming extensive breakdown of the native lignin matrix. In parallel, a pronounced increase in lignin molecular weight was observed, rising from an initial 3160 to 4335 Da after 1 h, 9397 Da after 2 h, and ultimately reaching 20800 Da after 3 h. This remarkable molecular weight growth clearly indicates intensive self-condensation (esterification) reactions yielding high-molecular-weight macromolecular structures. Quantitative ^{31}P NMR further supported this interpretation by showing a rapid depletion of aliphatic −OH groups, decreasing from 2.99 to 1.20 mmol/g after 1 h, 0.35 mmol/g after 2 h, and 0.29 mmol/g after 3 h. The carboxylic −OH content first increased from 0.02 to 0.09 mmol/g within the initial hour, and 0.11 mmol/g after 2 h (under 150 °C), but subsequently decreased to 0.06 mmol/g and remained unchanged thereafter. In contrast, phenolic −OH groups were strongly reduced during the first hour, dropping from 2.13 mmol/g to 0.89 mmol/g, and further diminished to 0.48 mmol/g by the second hour before stabilizing. The simultaneous loss of both aliphatic and phenolic hydroxyl functionalities is consistent with extensive condensation and rearomatization reactions, which consume reactive lignin functionalities. As evident from Figure 9, the declining $S_{2/6}$, G_2, and G_6 cross-signal intensity and selective

https://doi.org/10.1021/acssuschemeng.6c00430
ACS Sustainable Chem. Eng. 2026, 14, 8685−8700

carboxylation at $S_{2/6}$, G_2, and G_6 positions together indicate modification of both S and G units during the early stages of the reaction. The collapse of the β-O-4 ether network, combined with the disappearance of other interunit bonds, confirms that depolymerization precedes condensation. Such a depolymerization/recondensation sequence is characteristic of lignin thermal processing. Once β-O-4 bonds are cleaved, highly reactive phenolic and benzylic intermediates are formed, which rapidly undergo intermolecular C−C coupling,[40] leading to molecular weight growth and reduced solubility. The observed Mw increase from 3160 to 20,800 Da therefore reflects chemical cross-linking rather than mere particle aggregation. These findings indicate that under the investigated conditions, condensation reactions compete strongly with CO_2 incorporation. After this initial cleavage phase, rearrangement processes dominate and promote rapid molecular growth through C−C bond formation. Collectively, the NMR and SEC data reveal an initial stage characterized by β-O-4 cleavage and selective −COOH introduction, followed by rapid self-condensation (esterification) yielding a highly cross-linked, high-molecular-weight lignin. Collectively, these results demonstrate that, although initial carboxylation occurs at specific positions, it is rapidly overtaken by extensive depolymerization and subsequent condensation reactions, which dominate the overall transformation of lignin.

In addition to the alkali additive effect, the presence and abundance of various functional groups, as well as the overall molecular structure, can contribute to lignin's condensation. Therefore, the choice of lignin's isolation procedure can also be detrimental to its potential further upgrading. Perhaps Kraft lignin would show an increased extent of carboxylation, as during its processing with sodium hydroxide, an increased content of phenolic hydroxyl groups is evident; however, its high sulfur content may play a detrimental role in activity, selectivity, and potential further separation and purification processes. On the other hand, fractionation of lignin to obtain fragments with various molecular weight fractions may also play a role. As the literature shows, in the organosolv method, while adjusting the ratio between the solvent and antisolvent, it is possible to obtain low-molecular-weight lignin fractions with higher amounts of phenolic −OH groups.[36] Overall, the choice of lignin isolation and pretreatment could be adjusted for selective isolation of lignin fragments, thus selecting its physicochemical characteristics to be more compatible with more efficient lignin carboxylation.

From a process perspective, these findings demonstrate that direct lignin carboxylation is strongly limited under the investigated conditions. Although partial CO_2 incorporation occurs, as evidenced by the increase in −COOH content from 0.02 to 0.09−0.11 mmol g^{-1}, the process is rapidly dominated by thermally induced condensation and repolymerization reactions. These lead to a decrease in hydroxyl group content, a substantial increase in molecular weight up to 20,800 Da, and eventual loss of solubility. As a result, direct lignin carboxylation cannot be considered an effective or practically viable pathway under the conditions studied. However, the measurable incorporation of CO_2 and formation of carboxylic functionalities clearly demonstrate that direct functionalization of lignin is chemically possible. This observation indicates that with appropriate control of reaction pathways, improved catalytic systems, or optimized reaction conditions, more efficient direct lignin carboxylation may be achievable. Therefore, further investigation aimed at suppressing condensation reactions and enhancing selective CO_2 incorporation is required. In contrast to lignin-derived model compounds, the inherent structural complexity and reactivity of lignin promote competing pathways that suppress selectivity under the present conditions.

4. CONCLUSIONS

Lignin represents the most abundant natural source of aromatic compounds; thus, enhancing its valorization is crucial for improving the economic viability of biorefineries. Through selective depolymerization methods, it is possible to obtain various aromatic compounds, which can play a role in various industries. On the other hand, CO_2 utilization practices are in constant search for new technologies and chemical routes for its valorization. These two green-chemistry worlds, combined, represent huge potential for sustainable, environmentally friendly, and clean production of industrially relevant products. This study has proven that the traditional Kolbe-Schmitt-type carboxylation, with Marasse method alteration, can be an effective path for carboxylation of various lignin-derived aromatics. Compounds such as hydroxybenzene (phenol), dihydroxybenzenes (catechol, resorcinol, and hydroquinone), methylphenols (*o*-, *m*-, and *p*-cresols), methoxyphenols (guaiacol, 4-methylphenol, and syringol), and alkylphenols (4-propylphenol, eugenol, and 2-methoxy-4-propylphenol) could be successfully converted to their mono- or dicarboxylated corresponding aromatics. This study, for the first time, reported such an extensive array of hydroxybenzenes, systematically investigating the effect of various temperatures (150 and 200 °C) and reaction durations (1, 2, and 3 h) on their conversion and selectivity. Additionally, by investigating the first step of the Kolbe-Schmitt method, it was found that the successful preparation of metal phenoxide salts from these hydroxybenzenes requires specific and individually tailored conditions, thus confirming the superiority and efficient Marasse carboxylation method, using K_2CO_3 as an active base. Carboxylation of these hydroxybenzenes has led to the formation of various mono- and dicarboxylated hydroxybenzenes, which find their role in various industries (pharmaceutical, dyes, resins, polymers). Lastly, this study, also for the first time, demonstrates that direct incorporation of CO_2 into lignin is possible under mild conditions (150 °C, 2 h, 30 bar of CO_2), as evidenced by the increase in carboxylic functionalities. However, this process is accompanied by significant competing condensation and repolymerization reactions, which limit the extent of functionalization and prevent it from being an effective pathway under the investigated conditions. This study, comprehensively, has provided the research society with the foundation to expand future studies on the carboxylation of lignin-derived aromatics.

Importantly, this study first establishes a rapid and systematic screening platform for lignin-derived aromatics by employing the Marasse carboxylation methodology, thereby omitting the need for preformed metal phenoxides required in the classical Kolbe−Schmitt approach. This in situ carbonate-mediated strategy enabled consistent comparison across 14 structurally diverse substrates and allowed for efficient evaluation of intrinsic structure−reactivity relationships. While this approach provides a robust benchmarking framework, it should be acknowledged that individually optimized preformed metal phenoxides may potentially afford higher yields and/or altered regioselectivity and product distributions. Within this unified methodology, clear trends emerged: the

https://doi.org/10.1021/acssuschemeng.6c00430
ACS Sustainable Chem. Eng. 2026, 14, 8685−8700

electronic nature of aromatic substituents, the relative orientation and availability of phenolic −OH groups, and steric constraints were found to govern conversion and selectivity, thereby offering a predictive basis for designing biomass-derived aromatics suitable for CO_2 upgrading.

Furthermore, this work demonstrates that structurally diverse lignin-derived aromatics can undergo direct CO_2 incorporation under moderate pressures (30 bar) and comparatively mild temperatures (150−200 °C), expanding the practical scope of carbonate-mediated carbon fixation beyond classical phenol substrates. The successful conversion to mono- and dicarboxylated aromatic acids highlights a viable pathway toward value-added building blocks relevant to pharmaceuticals, polymer precursors, resins, and specialty chemicals, directly linking lignin valorization to carbon utilization strategies. In addition, the proof-of-concept demonstration of direct lignin functionalization indicates that CO_2 incorporation into the lignin structure is chemically possible, although it remains limited under the investigated conditions due to competing condensation pathways. These findings suggest that while direct carboxylation without prior depolymerization is not yet a viable approach, it represents a promising direction that requires further investigation and optimization. Potential future research should investigate the effect of various reaction conditions and find the most optimal ones for each reaction individually. The research society, as well as industry, could benefit from the extensive and systematic investigation of the effect of various reaction conditions on the conversion of these hydroxybenzenes, as well as the selectivity to various industrially relevant mono- and dicarboxylated lignin-derived aromatics.

■ ASSOCIATED CONTENT

Supporting Information

The Supporting Information is available free of charge at https://pubs.acs.org/doi/10.1021/acssuschemeng.6c00430.

List of ^{1}H chemical shifts of all observed products; schemes of all investigated reactants with theoretical and experimentally obtained carboxylation products; list of all carboxylation reaction conditions, names, and yields of obtained mono- and dicarboxylated products (PDF)

■ AUTHOR INFORMATION

Corresponding Authors

Blaž Likozar − *Department of Catalysis and Chemical Reaction Engineering, National Institute of Chemistry, 1000 Ljubljana, Slovenia; Faculty of Polymer Technology, SI-2380 Slovenj Gradec, Slovenia;* orcid.org/0000-0001-7226-4302; Email: blaz.likozar@ki.si

Miha Grilc − *Department of Catalysis and Chemical Reaction Engineering, National Institute of Chemistry, 1000 Ljubljana, Slovenia; University of Nova Gorica, 5000 Nova Gorica, Slovenia;* orcid.org/0000-0002-8255-647X; Email: miha.grilc@ki.si

Authors

Aleksa Kojčinović − *Department of Catalysis and Chemical Reaction Engineering, National Institute of Chemistry, 1000 Ljubljana, Slovenia; University of Nova Gorica, 5000 Nova Gorica, Slovenia*

Marko Gabrovšek − *Department of Catalysis and Chemical Reaction Engineering, National Institute of Chemistry, 1000 Ljubljana, Slovenia*

Edita Jasiukaitytė-Grojzdek − *Department of Catalysis and Chemical Reaction Engineering, National Institute of Chemistry, 1000 Ljubljana, Slovenia;* orcid.org/0000-0001-9065-5761

Complete contact information is available at: https://pubs.acs.org/10.1021/acssuschemeng.6c00430

Author Contributions

A.K.—Data curation, formal analysis, investigation, methodology, visualization, writing—original draft; M.G.—Data curation and formal analysis; E.J.G.—Data curation, formal analysis, writing—original draft; B.L.—Conceptualization, funding acquisition, project administration, resources, supervision; M.G—Funding acquisition, methodology, resources, supervision, validation, writing—review and editing.

Funding

The authors would like to acknowledge the financial support of the Slovenian Research Agency (Core Funding P2−0152 and Grant No. J2−1723 and J2−2492).

Notes

The authors declare no competing financial interest.

■ REFERENCES

(1) Sassoli, D. M.; Fernandes, J. P. M. *Sustainable Finance and Climate Change: Law and Regulation*; The European Parliament and the Council of the European Union, 2021; pp 116−136.

(2) Galkin, M. V.; Samec, J. S. M. Selective Route to 2-Propenyl Aryls Directly from Wood by a Tandem Organosolv and Palladium-Catalysed Transfer Hydrogenolysis. *ChemSusChem* **2014**, *7* (8), 2154−2158.

(3) Alassmy, Y. A.; Pour, Z. A.; Pescarmona, P. P. Efficient and Easily Reusable Metal-Free Heterogeneous Catalyst Beads for the Conversion of CO2 into Cyclic Carbonates in the Presence of Water as Hydrogen-Bond Donor. *ACS Sustainable Chem. Eng.* **2020**, *8* (21), 7993−8003.

(4) Isikgor, F. H.; Becer, C. R. Lignocellulosic Biomass: A Sustainable Platform for the Production of Bio-Based Chemicals and Polymers. *Polym. Chem.* **2015**, *6* (25), 4497−4559.

(5) Belluati, M.; Tabasso, S.; Gaudino, E. C.; Cravotto, G.; Manzoli, M. Biomass-Derived Carbon-Based Catalysts for Lignocellulosic Biomass and Waste Valorisation: A Circular Approach. *Green Chem.* **2024**, *26*, 8642−8668, DOI: 10.1039/d4gc00606b.

(6) Zhao, W.; Ge, Q.; Li, H.; Jiang, N.; Yang, S.; Cong, H. Catalyst-Free Valorization of Biomass Resources to Value-Added Products. *Green Chem.* **2024**, 8550−8563, DOI: 10.1039/d4gc01541j.

(7) Zhang, X.; Ma, H.; Wu, S. Effects of Temperature and Atmosphere on the Formation of Oligomers during the Pyrolysis of Lignin. *Fuel* **2020**, *268*, No. 117328.

(8) Mahmood, N.; Yuan, Z.; Schmidt, J.; Xu, C. Production of Polyols via Direct Hydrolysis of Kraft Lignin: Effect of Process Parameters. *Bioresour. Technol.* **2013**, *139*, 13−20.

(9) Lang, M.; Li, H. Toward Mild Synthesis of Functional Chemicals from Lignin-Derived Phenolics via Emerging Catalytic Technology. *Chem. Catal.* **2023**, *3* (5), No. 100609.

(10) Wang, S.; Zhang, K.; Li, H.; Xiao, L. P.; Song, G. Selective Hydrogenolysis of Catechyl Lignin into Propenylcatechol over an Atomically Dispersed Ruthenium Catalyst. *Nat. Commun.* **2021**, *12* (1), No. 416.

(11) Ročnik, T.; Likozar, B.; Jasiukaitytė-Grojzdek, E.; Grilc, M. Catalytic Lignin Valorisation by Depolymerisation, Hydrogenation, Demethylation and Hydrodeoxygenation: Mechanism, Chemical

Reaction Kinetics and Transport Phenomena. *Chem. Eng. J.* **2022**, *448*, No. 137309.
(12) Radhika, N. L.; Sachdeva, S.; Kumar, M. Lignin Depolymerization and Biotransformation to Industrially Important Chemicals/Biofuels. *Fuel* **2022**, *312*, No. 122935.
(13) Martínková, L.; Grulich, M.; Pátek, M.; Křístková, B.; Winkler, M. Bio-Based Valorization of Lignin-Derived Phenolic Compounds: A Review. *Biomolecules* **2023**, *13* (5), No. 717.
(14) Jérôme, F.; Luque, R.*Bio-Based Solvents*; Wiley, 2017 DOI: 10.1002/9781119065357.
(15) Schmitt, R. Beitrag Zur Kenntniss Der Kolbe'schen Salicylsäure Synthese. *J. Prakt. Chem.* **1885**, *31* (1), 397−411.
(16) Baine, O.; Adamson, G. F.; Barton, J. W.; Fitch, J. L.; Swayampati, D. R.; Jeskey, H. A Study of the Kolbe-Schmitt Reaction. II. The Carbonation of Phenols. *J. Org. Chem.* **1954**, *19* (4), 510−514.
(17) Cameron, D.; Jeskey, H.; Baine, O. The Kolbe-Schmitt Reaction. I. Variations in the Carbonation of p-Cresol. *J. Org. Chem.* **1950**, *15* (2), 233−236.
(18) Rahim, M. A.; Matsui, Y.; Kosugi, Y. Effects of Alkali and Alkaline Earth Metals on the Kolbe-Schmitt Reaction. *Bull. Chem. Soc. Jpn.* **2002**, *75* (3), 619−622.
(19) Marković, Z.; Markovic, S.; Begovic, N. Influence of Alkali Metal Cations upon the Kolbe-Schmitt Reaction Mechanism. *J. Chem. Inf. Model.* **2006**, *46* (5), 1957−1964.
(20) Iijima, T.; Yamaguchi, T. The Improved Kolbe-Schmitt Reaction Using Supercritical Carbon Dioxide. *Tetrahedron Lett.* **2007**, *48* (30), 5309−5311.
(21) Mohammad, O.; Onwudili, J. A.; Yuan, Q.; Evans, R. Advancing CO2 Utilisation via Suspension-Based Carboxylation of Single and Mixed Biomass-Derived Phenolics to Produce High-Value Hydroxybenzoic Acids. *Chem. Eng. J.* **2025**, *515*, No. 163498.
(22) Kojčinović, A.; Likozar, B.; Grilc, M. Sustainable CO 2 Fixation onto Bio-Based Aromatics. *Sustainability* **2023**, *15*, No. 16321.
(23) Kojčinović, A.; Likozar, B.; Grilc, M. Mechanism, Kinetics and Modelling of Phenol Carboxylation Reactions with CO2. *Int. J. Mol. Sci.* **2024**, *25* (23), No. 12923.
(24) Tran, F.; Lancefield, C. S.; Kamer, P. C. J.; Lebl, T.; Westwood, N. J. Selective Modification of the β-β Linkage in DDQ-Treated Kraft Lignin Analysed by 2D NMR Spectroscopy. *Green Chem.* **2015**, *17* (1), 244−249.
(25) Lindsey, A. S.; Jeskey, H. The Kolbe-Schmitt Reaction. *Chem. Rev.* **1957**, *57* (4), 583−620.
(26) Shanthi, B.; Palanivelu, K. Conversion of Carbon Dioxide to Resorcylic Acid under Ultrasonication by Kolbe-Schmitt Reaction. *Ultrason. Sonochem.* **2015**, *27* (1), 268−276.
(27) Krtschil, U.; Hessel, V.; Kost, H. J.; Reinhard, D. Kolbe-Schmitt Flow Synthesis in Aqueous Solution - From Lab Capillary Reactor to Pilot Plant. *Chem. Eng. Technol.* **2013**, *36* (6), 1010−1016.
(28) Barbarossa, V.; Barzagli, F.; Mani, F.; Lai, S.; Vanga, G. The Chemistry of Resorcinol Carboxylation and Its Possible Application to the CO2 Removal from Exhaust Gases. *J. CO2 Util.* **2015**, *10*, 50−59.
(29) Payer, S. E.; Marshall, S. A.; Bärland, N.; Sheng, X.; Reiter, T.; Dordic, A.; Steinkellner, G.; Wuensch, C.; Kaltwasser, S.; Fisher, K.; Rigby, S. E. J.; Macheroux, P.; Vonck, J.; Gruber, K.; Faber, K.; Himo, F.; Leys, D.; Pavkov-Keller, T.; Glueck, S. M. Regioselective Para-Carboxylation of Catechols with a Prenylated Flavin Dependent Decarboxylase. *Angew. Chem., Int. Ed.* **2017**, *56* (44), 13893−13897.
(30) Yoshida, T.; Inami, Y.; Matsui, T.; Nagasawa, T. Regioselective Carboxylation of Catechol by 3,4-Dihydroxybenzoate Decarboxylase of Enterobacter Cloacae P. *Biotechnol. Lett.* **2010**, *32* (5), 701−705.
(31) Hessel, V.; Hofmann, C.; Löb, P.; Löwe, H.; Parals, M. Microreactor Processing for the Aqueous Kolbe-Schmitt Synthesis of Hydroquinone and Phloroglucinol. *Chem. Eng. Technol.* **2007**, *30* (3), 355−362.
(32) Plasch, K.; Hofer, G.; Keller, W.; Hay, S.; Heyes, D. J.; Dennig, A.; Glueck, S. M.; Faber, K. Pressurized CO2 as a Carboxylating Agent for the Biocatalytic: Ortho -Carboxylation of Resorcinol. *Green Chem.* **2018**, *20* (8), 1754−1759.
(33) Ji, Y.; Yao, Q.; Zhao, Y.; Cao, W. On the Origin of Alkali-Catalyzed Aromatization of Phenols. *Polymers* **2019**, *11* (7), No. 1119.
(34) Peng, C.; Liu, Y.; Guo, X.; Liu, W.; Li, Q.; Zhao, Z. K. Selective Carboxylation of Substituted Phenols with Engineered *Escherichia Coli* Whole-Cells. *Tetrahedron Lett.* **2018**, *59* (42), 3810−3815.
(35) Sengoden, M.; Bhat, G. A.; Roland, T.; Hsieh, C. M.; Darensbourg, D. J. Facile Synthesis of Polycarbonates from Biomass-Based Eugenol: Catalyst Optimization for Selective Copolymerization of CO2 and Eugenol to Achieve Polycarbonates. *RSC Sustainable* **2024**, *2* (5), 1431−1443.
(36) Jasiukaityte-Grojzdek, E.; Kozmelj, T. R.; Tofani, G.; Segers, B.; Nimmegeers, P.; Billen, P.; Pogorevc, R.; Likozar, B.; Grilc, M. Design of Organosolv Lignin Fractionation: Influence of Temperature, Antisolvent, and Source on Molecular Weight, Structure, and Functionality of Lignin Fragments. *ACS Sustainable Chem. Eng.* **2025**, *13* (9), 3452−3466.
(37) Jasiukaityte-Grojzdek, E.; Huš, M.; Grilc, M.; Likozar, B. Acid-Catalysed α-O-4 Aryl-Ether Bond Cleavage in Methanol/(Aqueous) Ethanol: Understanding Depolymerisation of a Lignin Model Compound during Organosolv Pretreatment. *Sci. Rep.* **2020**, *10*, No. 11037.
(38) Kawamoto, H. Lignin Pyrolysis Reactions. *J. Wood Sci.* **2017**, *63*, 117−132.
(39) Yin, L.; Leng, E.; Gong, X.; Zhang, Y.; Li, X. Journal of Analytical and Applied Pyrolysis Pyrolysis Mechanism of β-O-4 Type Lignin Model Polymers with Different Oxygen Functional Groups on Cα. *J. Anal. Appl. Pyrolysis* **2018**, *136*, 169−177.
(40) Nakamura, T.; Kawamoto, H.; Saka, S. Condensation Reactions of Some Lignin Related Compounds at Relatively Low Pyrolysis Temperature. *J. Wood Chem. Technol.* **2007**, *27* (2), 121−133.
(41) Li, J.; Bai, X.; Dong, Z.; Chen, Y.; Yang, H.; Wang, X.; Chen, H. Influence of Additives on Lignin Agglomeration and Pyrolysis Behavior. *Fuel* **2020**, *263*, No. 116629.
(42) Su, Y.; Zhang, S.; Xiong, Y.; Zhang, H. Detecting the Inner Mechanism of Agglomeration Behaviors and Product Properties during Fast Pyrolysis of Lignin via Alkaline Additives. *Fuel Process. Technol.* **2022**, *238*, No. 107528.

https://doi.org/10.1021/acssuschemeng.6c00430
ACS Sustainable Chem. Eng. 2026, 14, 8685−8700